UMEÅ UNIVERSITY

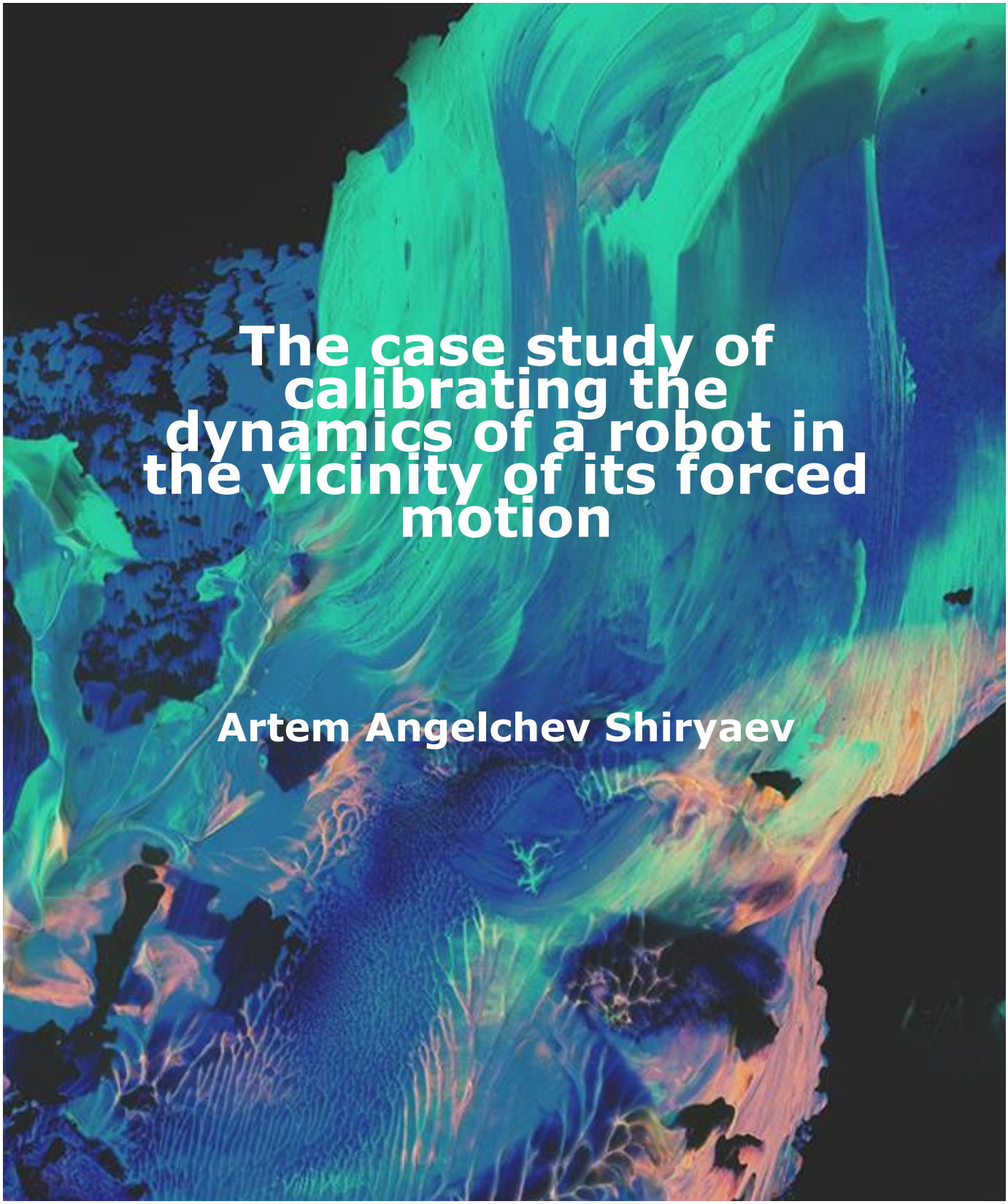

The case study of calibrating the dynamics of a robot in the vicinity of its forced motion

Artem Angelchev Shiryaev

Master thesis, 30 ECTS

Master of Science in Mathematical Statistics, 120 ECTS

Autumn 2024

[This page was intentionally left blank]

The Case Study of Calibrating the Dynamics of a Robot in the Vicinity of its Forced Motion

Artem Angelchev Shiryaev

Master of Science in Mathematical Statistics
Department of Mathematics
and Mathematical Statistics
Umeå University
Autumn 2024

[This page was intentionally left blank]

Abstract

This thesis investigates the calibration of the dynamics of a robotic system. Using a case study of the Butterfly robot, an educational robotic setup developed by Robotikum AB, the study aims to identify and recalibrate the parameters that define the robot's dynamics. The approach combines physics-driven and grey-box modeling to represent the robot's mechanical system. The dynamics are modeled using non-linear differential equations, and the parameters are estimated through grey-box methods and frequency response analysis.

Experimental data, gathered through simulations in Simulink and real-world tests collected from the Butterfly robot, are used to validate the model, focusing on the robot's first degree of freedom, which represents the rotation of the robotic hand. The study further explores recalibration methods in the vicinity of a forced motion, discussing both theoretical foundations and practical application. The results contribute to the development of more accurate estimates showcased on the Butterfly Robot case study.

keywords: Robotics, Butterfly Robot, Simulation, Control, Statistics, grey-box models.

Contents

1 Introduction

Developing robotic systems with advanced functionalities requires tools for modeling and analyzing such systems. The classical insights into the problems rely on

- various methods of mechanics and engineering subjects aimed at reconstructing families of phenomenological, grey-box or physics driven models for capturing dynamics of a robotic system, which are written in a format(s) delineated and well-known up to a number of uncertain parameters; and
- various methods of statistics and optimization for recovering estimates for these parameters and selecting in this way one model that is mostly appropriate for describing the dynamics of a concrete physical robotic system.

Overall process of modeling and model calibration is multidisciplinary. It typically involves planning and organizing experimental studies on a robotic system, engages various technical and programming skills for collecting the data and takes advantages of mathematical tools for data processing, optimization and drawing conclusions. When successfully implemented, the mentioned steps result in a calibrated mathematical model and its software realization that can be used for

- planning new (forced) motions of the robotic system,
- developing and testing feedback control architectures for demonstrating occurrences of such motions of the robotic system in nominal and varied conditions,
- detecting abnormal (faulty) behaviours of the robotic system,
- predicting and exploring new functionalities of the robotic system if some of its software components and hardware subsystems are changed to new ones, *etc.*

However, most of the derived models are *generic*; that is, they are universal and of use for general purposes. Indeed, often by construction, they have abilities to predict and approximately resemble responses of physical systems to any control input or any disturbance well *on average*, see [8, 7, 1, 4] and many others.

Meanwhile, in applications, robots are typically anticipated to perform a few specific motions until they are reprogrammed to new scenario of work

to perform new set of a few specific motions, *ect.* This observation indicates that any of such *generic* models prior to be used in applications **requires re-tuning and re-calibrating parameters of the model** for improving its accuracy in representing the dynamics of the robotic system **in a vicinity of a particular forced motion.**

The thesis can be seen as a probe step into that direction and examines the problem for the particular robotic system – the so-called "Butterfly" robot – created as new educational set-up for illustrating basic and advanced control and robotics laboratory exercises by Robotikum AB, see Fig. 1. The robot is consisting of two components:

- a "robotic hand" with the surface resembling a figure-eight shape, which can rotate about a fixed axis and which behavior can be directly controlled by a DC-motor; and
- a passive ball that can freely roll on the boundary of the "robotic hand," which motions are driven only by the gravity applied at the center of mass of the ball, and reaction and friction forces applied at the point of contact, i.e. where the ball touches the "robotic hand."

In the thesis, we will start with exploring, commenting and analyzing the data collected for calibrating the dynamics of the first degree of freedom of the robot, i.e. the dynamics of the "robot hand" and the rotor of the DC-motor connected firmly to each other by the clutch and considered as one rigid body rotating about the fixed axis. Namely, we will first

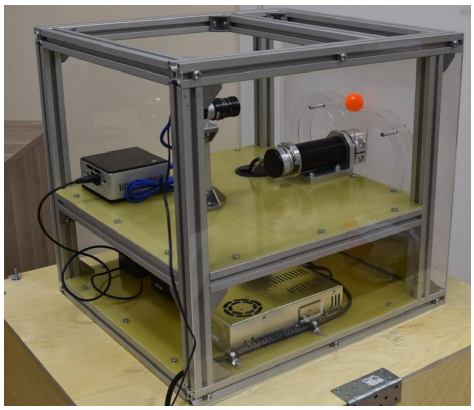

Figure 1: The Butterfly robot: the system consists of the "robot-hand" controlled by a DC-motor and the ball that can freely roll on the hand.

- provide the physics driven and grey-box models of the dynamics of the 1-st degree of freedom of the robotic system;

- repeat and comment arguments commonly used for identification of lumped parameters of such models processing "synthetic" data generated through simulation of various responses of the model of the robotic system; and, then,

- apply these methods for computing estimates of the parameters of a *generic* model of the dynamics of the *physical* robotic system.

When these steps completed and commented, we turn to the main problem of the thesis and discuss the novel approach and computational methods for re-calibration of the system dynamics in a vicinity of a particular (forced) motion of the robotic system.

1.1 Modeling the robot under study

For the robotic system under study, its model should primarily represent and capture the dynamics of a planar system consisting of several rigid bodies firmly attached to each other, and which altogether (i.e. as one rigid body) rotate in the vertical plane about one fixed axis driven primarily by the gravity, by the friction at the pivot and by the external torque generated by the DC-motor. The dynamics of the mechanical part of that system, see Fig. 2, can be written

- either in excessive coordinates $(x; y)$; or

- with the help of one generalized coordinate – a scalar variable θ denoting the angle of inclination of the line passing through the pivot and the centre of mass of the rigid body from the vertical, see Fig. 2; here the positive direction of the angle θ is counted anti-clockwise.

The last choice of the coordinates results in the equations of lower order with smaller number of parameters, so that it is followed next. Taking advantage of the Lagrange formalism, the dynamics of the system is described by the Euler-Lagrange equation

$$\frac{d}{dt}\left[\frac{\partial L(\theta,\dot{\theta})}{\partial \dot{\theta}}\right] - \frac{\partial L(\theta,\dot{\theta})}{\partial \theta} = \sum_k \tau_k, \tag{1}$$

where τ_k represent external torques applied to the system and where $L(\theta,\dot{\theta})$ is the Lagrangian of the system defined as a difference between its kinetic and potential energies:

$$L(\cdot) := K(\cdot) - P(\cdot).$$

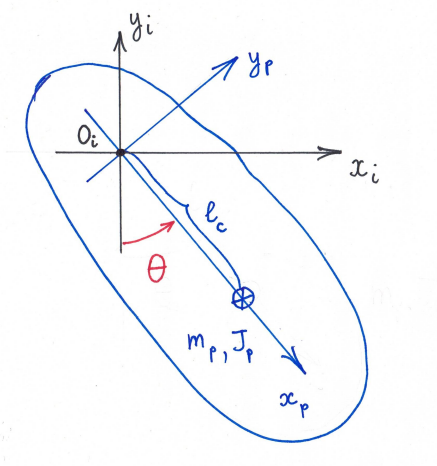

Figure 2: Coordinates for defining a rigid body rotation in the vertical plane about fixed axis. They are either excessive coordinates $(x; y)$ of the centre of mass of the rigid body, or it is the generalized coordinate θ defined as the angle between the vertical and the line passing through the pivot and the centre of mass, which positive direction is counted anti-clockwise.

For the planar system with one revolute joint depicted on Fig. 2, these functions are of the form

$$\begin{aligned} K(\cdot) &:= \tfrac{1}{2} m_p \left(\dot{x}^2 + \dot{y}^2\right) + \tfrac{1}{2} J_p \dot{\theta}^2 = \tfrac{1}{2} \left(m_p l_c^2 + J_p\right) \dot{\theta}^2 \\ P(\cdot) &:= m_p g y = -\, m_p g l_c \cos\theta \end{aligned}$$

Here m_p is the mass of the rigid body, l_c is the distance from the pivot to its centre of mass, J_p is the moment of inertia of the link about its centre of mass, and g is the acceleration due to gravity. With the mentioned above $K(\cdot)$ and $P(\cdot)$, the Euler-Lagrange equation (1) defines the dynamics of the mechanical part of the robotic system written as one second order nonlinear differential equation with an external input

$$\left[J_p + m_p l_c^2\right] \cdot \ddot{\theta}(t) + m_p g l_c \cdot \sin\big(\theta(t)\big) = \tau_u(t) + \tau_{ex}(t). \tag{2}$$

Such an input – the right-hand side of Eqn. (2) – is a sum of external generalized torques, where

- $\tau_u(\cdot)$ is a torque generated by the DC-motor to rotate the rigid body about the fixed axis; and
- $\tau_{ex}(\cdot)$ is a sum of external torques due to other physics phenomenon affecting the process such as friction at the joint, backlash due to loose

connection and/or misalignment of the rotation axes of the rotor and the "robot hand" connected by the clutch, and *etc.*

For the case study, we can start with the simplest guess and approximate the torque $\tau_{ex}(\cdot)$ as a sum of a linear viscous friction and a minor (non-modelled) part $\tau_{\varepsilon}(\cdot)$ of *unknown nature,* i.e.

$$\tau_{ex}(t) = -k_f \cdot \tfrac{d}{dt}\theta(t) + \tau_{\varepsilon}(t), \qquad k_f > 0. \tag{3}$$

Beside the model of the dynamics of the mechanical sub-system of the robot, the simplest physics driven model of the dynamics of its electrical sub-system is commonly considered of the form

$$\tau_u(t) = k_i \cdot i(t), \quad L \cdot \tfrac{d}{dt} i(t) + R \cdot i(t) = v(t) - k_{emf} \cdot \tfrac{d}{dt}\theta(t), \tag{4}$$

where

$i(\cdot)$ is a armature current of the DC-motor;

$v(\cdot)$ is a voltage (control signal) applied to the DC-motor;

$k_{emf} \cdot \frac{d}{dt}\theta(\cdot)$ represents a model of the so-called *back electromotive force*, which is a voltage that occurs in electric motors, when there is a relative motion between the armature and the magnetic field produced by the motor's field coils;

L, R, k_i are positive constant values of the motor's inductance, resistance and torque gain.

Eqns. (2)-(4) can be seen as a **physics-based approximation** of the dynamics of the robotic system under study. Such mathematical model comprises a nonlinear differential equation, which depends on a number of constant parameters and which has

- three internal states consisting of the shaft's angle, its rate of change and the armature current, i.e. $\big[\theta(\cdot); \dot{\theta}(\cdot); i(\cdot)\big]$;
- a scalar control input constituting an external voltage applied to the DC-motor $v(\cdot)$;
- a scalar output (measured signal) – the shaft's angle $\theta(\cdot)$.

Under the common assumption that the motor's inductance L is very small, $L \approx 0$, a *generic* **grey-box parametric model** of dynamics of the robotic system takes the reduced order form

$$p_1 \cdot \ddot{\theta}(t) + p_2 \cdot \dot{\theta}(t) + p_3 \cdot \sin\big(\theta(t)\big) = p_4 \cdot v(t) + \tau_{\varepsilon}(t), \tag{5}$$

where the control variable $v(\cdot)$ is a voltage applied to the DC-motor; and the listed coefficients p_1-p_4 are positive and determined by physical parameters of the robot as follows

$$p_1 := J_p + m_p l_c^2, \quad p_2 := k_f + k_{emf} \cdot \frac{k_i}{R}, \quad p_3 := m_p g l_c, \quad p_4 := \frac{k_i}{R}. \tag{6}$$

The standard assignment of identification of parameters of the model (5) for the robotic system is decomposed into several sub-tasks. Namely,

1. to plan one or several control inputs $v_k(t)$, $k = 1, \ldots, N$, each defined as a continuous-in-time signal on time interval $[0, T_k]$;

2. to organize a series of experiments and record responses of the system to such inputs $v_k(\cdot)$, $k = 1, \ldots, N$. Typically, the recorded data comprise the sampled behavior(s) of the coordinate $\theta_k(t)$ that becomes measured for the time interval $[0, T_k]$ of the corresponding control signal(s);

3. to process the recorded data and compute estimates $\hat{p}_i$ for the lumped parameters p_1-p_4 of the dynamic system (5), and further, if possible, provide estimates for some of its physical parameters. For the case study and according to Eqn. (6), they are

$$\hat{J}_p, \quad \hat{m}_p, \quad \hat{l}_c, \quad \hat{k}_f, \quad \hat{k}_i, \quad \hat{R}, , \quad \hat{k}_{emf}; \tag{7}$$

4. to provide extra insights on properties of non-modelled part of the dynamics, which for the case study can be re-phrased as to improve modelling of the external part of the input to the system denoted in Eqn. (3) as $\tau_\varepsilon(\cdot)$.

Remark 1 The control system (5) is a nonlinear second order differential equation with *linear format of dependence* of the dynamics on the lumped parameters p_1-p_4. If both the angular velocity $\dot{\theta}(t)$ and the angular acceleration $\ddot{\theta}(t)$ of the coordinate $\theta(t)$ would be measured, then Eqn. (5) can be re-written in the format of a linear regression, which could be consequently used both for estimating unknown parameters and for improving the representation of non-modelled part $\tau_\varepsilon(\cdot)$.

However, this approach might be considered as *naive*. Indeed, it would work if the model indeed covers the system's dynamics and allows predicting accurately the physical system behaviours by computing solutions of that nonlinear differential equation for extended time span. Unfortunately, this is not the case and appropriate comments and remarks will be done later in text. Furthermore, the signals $\dot{\theta}(t)$ and $\ddot{\theta}(t)$ cannot be directly measured in

the robotic application. So that organizing the identification of parameters in such *straightforward* manner can unlikely reach affirmative answers and serve the goal. ■

The mentioned limitation gives rise to alternative methods, and most of standard approaches for identification of the parameters of (5) are grounded on another type of "linearity" found for local representations of the process. Namely, they are comprising the steps of

1. developing and analyzing the linearization of the model of the nonlinear control system (5) in a vicinity of one of its stable equilibria;

2. reconstructing an estimate of the frequency response for the derived linear system;

3. and, finally, computing estimates for parameters of the nonlinear control system (5) based on the approximate frequency response of its linearization.

All of the sub-tasks 1.-3. above are explored and commented next, where in Section 2 we approach a synthetic model of the nonlinear control system (5) and advocate for some of useful steps and insights in processing the data. Later, in Section 3, we take advantage and apply the methods for calibrating parameters of the "real-world" robotic system and discuss the outcome of such work.

2 Reconstructing parameters of synthetic model's dynamics

2.1 Grey-box modeling and linearization

The grey-box model (5) of the robotic system is nonlinear and continuous-in-time. At first, we derive the linearization of the dynamics (5) about its stable equilibrium and, then, we convert that linear control system into a discrete-time format. The last step is required for analysis and identification procedures, if they are applied to sampled data that are collected in experiments run on the physical set-up.

Lemma 1 *Consider the nonlinear control system (5) and suppose the part of non-modelled dynamics $\tau_\varepsilon(\cdot)$ is negligible in a vicinity of its equilibrium θ_e at 0, then the linearization of the system (5) about that point is defined by*

$$p_1 \cdot \ddot{y}(t) + p_2 \cdot \dot{y}(t) + p_3 \cdot y(t) = p_4 \cdot u(t), \tag{8}$$

where the signals $y(\cdot)$ and $u(\cdot)$ represent variations of $\theta(\cdot)$ and $v(\cdot)$ from zero values provided that the signals $\theta(\cdot)$ and $v(\cdot)$ remain small enough. ■

Proof: If $\tau_\varepsilon(\cdot)$ can be dropped, then the state space model of the nonlinear system (5) with $\big[x_1 := \theta;\, x_2 := \dot{\theta}\big]$ has the form

$$\underbrace{\frac{d}{dt}\begin{bmatrix} x_1(t) \\ x_2(t) \end{bmatrix}}_{=:\,X} = \begin{bmatrix} x_2(t) \\ \frac{p_4}{p_1}\, v(t) - \frac{p_2}{p_1}\, x_2(t) - \frac{p_3}{p_1}\, \sin\big(x_1(t)\big) \end{bmatrix} =: \underbrace{\begin{bmatrix} f_1(\cdot) \\ f_2(\cdot) \end{bmatrix}}_{=:\,F(X)} + \underbrace{\begin{bmatrix} g_1(\cdot) \\ g_2(\cdot) \end{bmatrix}}_{=:\,G(X)} v$$

Standard arguments, see e.g. [6], suggest the format of the linearization of affine-in-control system

$$\dot{X} = F(X) + G(X)v$$

about its equilibrium at

$$x_{1e} = \theta_e = 0, \quad x_{2e} = \dot{\theta}_e = 0.$$

Namely, for the nonlinear control system above it is defined as an auxiliary linear control system of the form

$$\frac{d}{dt}\begin{bmatrix} \delta x_1(t) \\ \delta x_2(t) \end{bmatrix} = \begin{bmatrix} \frac{\partial f_1(\cdot)}{\partial x_1} & \frac{\partial f_1(\cdot)}{\partial x_2} \\ \frac{\partial f_2(\cdot)}{\partial x_1} & \frac{\partial f_2(\cdot)}{\partial x_2} \end{bmatrix}\Bigg|_{\substack{x_1=x_{1e} \\ x_2=x_{2e}}} \begin{bmatrix} \delta x_1(t) \\ \delta x_2(t) \end{bmatrix} + \begin{bmatrix} g_1(\cdot) \\ g_2(\cdot) \end{bmatrix}\Bigg|_{\substack{x_1=x_{1e} \\ x_2=x_{2e}}} u(t),$$

where the variables $\delta x_1(t)$ and $\delta x_2(t)$ as the first order approximates for deviations of the state vector components $x_1(t)$ and $x_2(t)$ from their values at the equilibrium

$$\delta x_1(t) \approx x_1(t) - x_{1e}, \qquad \delta x_2(t) \approx x_2(t) - x_{2e}.$$

For the case study the linearized state-space model of (5) is

$$\frac{d}{dt}\begin{bmatrix} \delta x_1(t) \\ \delta x_2(t) \end{bmatrix} = \begin{bmatrix} 0 & 1 \\ -\frac{p_3}{p_1} & -\frac{p_2}{p_1} \end{bmatrix} \begin{bmatrix} \delta x_1(t) \\ \delta x_2(t) \end{bmatrix} + \begin{bmatrix} 0 \\ \frac{p_4}{p_1} \end{bmatrix} u(t). \tag{9}$$

The system (9) can be re-written as (8) with $y(t) := \delta x_1(t)$. ■

The common method for identification of the parameters of (8) is based on analysis of frequency response of that linear control system and relies on the following general statement heavily used in engineering applications

Lemma 2 *Consider a stable single-input-single-output linear system described by the following differential equation*

$$\begin{aligned} a_n \tfrac{d^n}{dt^n} y(t) + a_{n-1} \tfrac{d^{n-1}}{dt^{n-1}} y(t) + \ldots + a_1 \tfrac{d}{dt} y(t) + a_0 y(t) \\ = \quad b_m \tfrac{d^m}{dt^m} u(t) + b_{m-1} \tfrac{d^{m-1}}{dt^{m-1}} u(t) + \cdots + b_1 \tfrac{d}{dt} u(t) + b_0 u(t) \end{aligned} \tag{10}$$

with $n \geq m$ and $\{a_i\}$, $\{b_i\}$ being real constants. Its response to the sinusoidal input signal

$$u(t) = A \cdot \sin\bigl(\omega_0 t\bigr), \quad \omega_0 > 0,$$

converges asymptotically to the steady-state oscillation

$$y_{ss}(t) = A \cdot \bigl|G(j\omega_0)\bigr| \cdot \sin\bigl(\omega_0 t + \varphi_0\bigr), \tag{11}$$

where the scalar rational function of complex variable $G(s)$ – called transfer function of the system (10) – is defined by differential equation (10) as follows

$$G(s) := \frac{b_m s^m + b_{m-1} s^{m-1} + \cdots + b_1 s + b_0}{a_n s^n + a_{n-1} s^{n-1} + \cdots + a_1 s + a_0} \tag{12}$$

and $\varphi_0 := arg\bigl\{G(j\omega_0)\bigr\}$. ■

Proof of the statement appears in the most of control oriented textbooks, e.g. [10, 5], and reflects an ability to compute the response of a linear control system to a sin-wave input analytically. The non-vanishing term of the response for the stable linear system (10) becomes equal to (11). ■

Remark 2 Frequency response of the linear control system (10) is defined as values of the corresponding transfer function $G(s)$ introduced for the system by Eqn. (12) for pure imaginary arguments, i.e. when $s = j\omega$ with ω being a real number varying from $-\infty$ to $+\infty$. ■

Remark 3 The transfer function (12) of the linear control system (8) has the form

$$G(s) := \frac{b_0}{a_2 s^2 + a_1 s + a_0} \tag{13}$$

with the coefficients of the numerator and the denominator well defined by constants p_1-p_4 but up to a common factor. Namely, any choice of coefficients

$$a_2 = \gamma \cdot p_1, \quad a_1 = \gamma \cdot p_2, \quad a_0 = \gamma \cdot p_3, \quad b_0 = \gamma \cdot p_4, \tag{14}$$

with γ being any non-zero constant, $\gamma \neq 0$, will be appropriate. Typically, the gain γ is chosen to be equal $\frac{1}{p_1}$. This preference makes the leading coefficient of the denominator to be equal one, while the others will be defined accordingly, i.e.

$$a_2 = 1, \quad a_1 = \frac{p_2}{p_1}, \quad a_0 = \frac{p_3}{p_1}, \quad b_0 = \frac{p_4}{p_1}.$$

The observation on non-uniqueness of parameters for (13) might preclude from a possibility to estimate all the parameters of the linearized dynamics (8). As a consequence, it might rule out a possibility to estimate all the parameters of the original nonlinear system (5) based on analysis of the transfer function (13). Nevertheless, the method of analysis of the linearization and its frequency response for identification of parameters of nonlinear dynamic systems is instrumental for use in engineering applications and will be examined further. ■

According to Lemma 2, exciting the linear second order control system with the transfer function (13) by the sinusoidal input

$$u(t) = A \cdot \sin\big(\omega t\big), \quad \omega > 0$$

results in the steady-state response of the form

$$y_{ss}(t) = A \cdot \big|G(j\omega)\big| \cdot \sin\big(\omega t + \varphi_0\big). \tag{15}$$

The factor of the amplitude of the response and its phase-shift are equal to

$$\big|G(j\omega)\big| = \sqrt{\big[\mathrm{Re}\,\{G(j\omega)\}\big]^2 + \big[\mathrm{Im}\,\{G(j\omega)\}\big]^2} \tag{16}$$

$$\tan(\varphi_0) = \frac{\mathrm{Im}\,\{G(j\omega)\}}{\mathrm{Re}\,\{G(j\omega)\}} \tag{17}$$

with the following components of real and imaginary parts of the complex-valued function $G(j\omega) = \mathrm{Re}\,\{G(j\omega)\} + j \cdot \mathrm{Im}\,\{G(j\omega)\}$ of $\omega \in \mathbb{R}^1$:

$$\mathrm{Re}\,\{G(j\omega)\} = \frac{b_0\big(a_0 - a_2\omega^2\big)}{\big(a_0 - a_2\omega^2\big)^2 + \big(a_1\omega\big)^2} = \frac{-\,p_4p_1 \cdot \omega^2 + p_4p_3}{p_1^2\omega^4 + \big(p_2^2 - 2p_1p_3\big)\omega^2 + p_3^2} \tag{18}$$

$$\mathrm{Im}\,\{G(j\omega)\} = \frac{-\,b_0a_1 \cdot \omega}{\big(a_0 - a_2\omega^2\big)^2 + \big(a_1\omega\big)^2} = \frac{-\,p_4p_2 \cdot \omega}{p_1^2\omega^4 + \big(p_2^2 - 2p_1p_3\big)\omega^2 + p_3^2} \tag{19}$$

Remark 4 The explicit format of the steady-state response (15)-(19) of the linear control system (8) to a sinusoidal signal is worthwhile. Indeed, according to Lemma 1, the steady-state response of the nonlinear system (5) is approximated by that function as well, i.e.

$$\theta_{ss}(t) \approx A \cdot \big|G(j\omega)\big| \cdot \sin\big(\omega t + \varphi_0\big) \tag{20}$$

provided that an amplitude A of the sinusoidal input signal

$$v(t) = A \cdot \sin\big(\omega t\big) \tag{21}$$

is chosen small enough. Selecting such a range of the amplitude A for different excitation frequencies of the control input (21) is determined during experiments' planning and recorded data processing. ■

2.2 Analysis of sampled data

Measurements of the signal $\theta(\cdot)$ for the nonlinear system (5) will be always sampled, i.e. the data available for analysis on time interval $[0, T]$ (sec) will be always given as a finite sequence of real numbers

$$\big\{\theta(t_k)\big\}_{k=0}^{k=N} = \big\{\theta(t_0),\ \theta(t_1),\ \theta(t_2),\ \ldots, \theta(t_N)\big\}, \quad \theta(t_k) \in \mathbb{R}^1, \tag{22}$$

where time instances t_k are strictly monotonically increasing

$$0 \approx t_0 < t_1 < t_2 < \cdots < t_k < \cdots < t_{N-1} < t_N \approx T.$$

Due to many reasons the time stamps – where the measurements are taken – might be varying in their increments, i.e.

$$\big(t_1 - t_0\big) \neq \big(t_2 - t_1\big) \neq \ldots \neq \big(t_{k+1} - t_k\big) \neq \ldots \neq \big(t_N - t_{N-1}\big).$$

For the same time interval of T seconds, a digital controller of the robot generates and sends to the DC-motor a sequence of control inputs

$$\big\{v(\tau_m)\big\}_{m=0}^{m=M} = \big\{v(\tau_0),\ v(\tau_1),\ v(\tau_2),\ \ldots, v(\tau_M)\big\}, \quad v(\tau_m) \in \mathbb{R}^1, \tag{23}$$

that will be reconstructed into the stair-case continuous-in-time function[1]

$$v_{zoh}(t) \equiv v(\tau_m), \quad \tau_m \leq t < \tau_{m+1}, \quad 0 = \tau_0 < \tau_1 < \cdots < \tau_M = T, \tag{24}$$

mimicking in this way the continuous-in-time input signal $v(\cdot)$ defined on that time interval.

Prior any further computations, the finite sequences of input and output signals

$$\big\{v.(\tau_k)\big\}_{m=0}^{m=M} \quad \text{and} \quad \big\{\theta(t_k)\big\}_{k=0}^{k=N}$$

available either as the recorded experimental data or as the data created by computer simulations – are often resampled and brought to the same constant sampling period of $\triangle$ (sec). When such pre-processing of the recorded data is realized, new vectors[2]

$$\begin{array}{rcl} \big\{v(k)\big\}_{k=1}^{k=N_c} & = & \big\{v(\triangle),\, v(2\triangle),\, \ldots,\, v(k\triangle),\, \ldots,\, v(N_c\cdot\triangle)\big\} \\ \big\{\theta(k)\big\}_{k=1}^{k=N_c} & = & \big\{\theta(\triangle),\, \theta(2\triangle),\, \ldots,\, \theta(k\triangle),\, \ldots,\, \theta(N_c\cdot\triangle)\big\} \end{array} \tag{25}$$

become reconstructed on approximately the same time interval $[0, T]$, where the original data were recorded, i.e. $N_c \cdot \triangle = T$.

There are several reasons for resampling the original data. For instance, if the sampling period is substantially smaller than the inverse of any possible rate of change of recorded signals, then most of recorded observations do not bear much information on the process. Therefore, the data are typically pre-processed and down-sampled changing the sampling period to larger value. Another reason to resample the data is to bring the finite sequences (22)-(24) to a common sampling period, *etc.*

The standard procedure for choosing a sampling period $\triangle$ appropriate for characterizing the system dynamics is based on analysis of *periodogram of Discrete Fourier transform (DFT)* of the sampled sequences (25), which we introduce next.

Definition 1 Given a vector with N_c-elements

$$\big\{w_k\big\}_{k=1}^{k=N_c} = \big\{w_1,\, w_2,\, \ldots,\, w_k,\, \ldots,\, w_{N_c}\big\},$$

originated from sampling a continuous-time signal $w(t)$ on a time interval $[0, T]$ at time instances $t_k = \triangle \cdot k$, $k = 1, \ldots, N_c$, i.e. $w_k := w(t_k)$ with

[1]The subscript 'ZOH' of the variable $v_{zoh}(\cdot)$ is the standard abbreviation for *Zero Order Hold* approximation of the original signal.

[2]Here we use the use the same names for reconstructed variables even though their values can differ from the values of these functions at mentioned time instances.

the sampling period $\triangle = \frac{T}{N_c}$, and given a vector $\{\Omega_k\}_{k=1}^{k=N_c}$ of N_c-frequencies spread equidistantly on the interval $(0, 2\pi]$

$$\{\Omega_1, \ldots, \Omega_k, \ldots, \Omega_{N_c}\} := \{\tfrac{2\pi}{N_c} \cdot 1, \ldots, \tfrac{2\pi}{N_c} \cdot k, \ldots, \tfrac{2\pi}{N_c} \cdot N_c\}, \tag{26}$$

the Discrete Fourier transform (DFT) of the finite sequence $\{w_k\}_{k=1}^{k=N_c}$ is the vector of complex numbers

$$\{W_k\}_{k=1}^{k=N_c} = \{W_1, W_2, \ldots, W_k, \ldots, W_{N_c}\}$$

defined by the linear transform of the vector $\{w_k\}_{k=1}^{k=N_c}$ and expressed in the component-wise form as follows

$$\begin{aligned} W_k &:= \frac{1}{\sqrt{N_c}}\big[w_1 \cdot e^{-j\cdot\Omega_1\cdot k} + \cdots + w_m \cdot e^{-j\cdot\Omega_m\cdot k} + \cdots + w_{N_c} \cdot e^{-j\cdot\Omega_{N_c}\cdot k}\big] \\ &= \frac{1}{\sqrt{N_c}} \sum_{m=1}^{N_c} w_m \cdot e^{-j\cdot\Omega_m\cdot k}, \qquad k = 1, \ldots, N_c \end{aligned} \tag{27}$$

The *periodogram* of the finite sequence $\{w_k\}_{k=1}^{k=N_c}$ is then defined as the vector of component-wise squared amplitudes of the vector $\{W_k\}_{k=1}^{k=N_c}$, i.e.

$$\Big\{|W_1|^2, |W_2|^2, \ldots, |W_k|^2, \ldots, |W_{N_c}|^2\Big\}, \tag{28}$$

where each component $|W_k|^2$ can be interpreted as the "weight" that the frequency $\Omega_k = \frac{2\pi}{N_c} \cdot k$, $k = 1, \ldots, N_c$, carries in the decomposition of the original data $\{w_k\}_{k=1}^{k=N_c}$. ■

Example 1 Let the signal $w(t)$ be a sinusoidal wave of frequency ω_0 $\left(\frac{rad}{sec}\right)$ and an amplitude $A > 0$, i.e.

$$w(t) = A \cdot \sin\big(\omega_0 \cdot t\big), \tag{29}$$

and let the continuous-time signal $w(t)$ be equidistantly sampled over the time interval $[0, T]$ at

$$t_1 = \tfrac{T}{N_c}, \quad t_2 = 2 \cdot \tfrac{T}{N_c}, \quad \ldots, \quad t_k = k \cdot \tfrac{T}{N_c}, \quad \ldots, \quad t_N = N_c \cdot \tfrac{T}{N_c} = T$$

resulting in the finite sequence of real numbers of size N_c

$$\begin{aligned} \{w_k\}_{k=1}^{k=N_c} &= \{w(t_1), w(t_2), \ldots, w(t_k), \ldots, w(t_{N_c})\} \\ &= \Big\{A \cdot \sin\big(\omega_0 \cdot 1 \cdot \tfrac{T}{N_c}\big), A \cdot \sin\big(\omega_0 \cdot 2 \cdot \tfrac{T}{N_c}\big), \ldots, \\ &\qquad A \cdot \sin\big(\omega_0 \cdot k \cdot \tfrac{T}{N_c}\big), \ldots, A \cdot \sin\big(\omega_0 \cdot N_c \cdot \tfrac{T}{N_c}\big)\Big\}. \end{aligned} \tag{30}$$

Since

$$\sin(\alpha) \equiv \tfrac{1}{2j}\left[e^{j\alpha} - e^{-j\alpha}\right], \quad \forall\, \alpha,$$

then by Eqns. (26)-(27) the components of the DFT of the finite sequence $\left\{w_k\right\}_{k=1}^{k=N_c}$ are created by sampling the sinusoidal wave are

$$\begin{aligned} W_k &= \frac{1}{\sqrt{N_c}} \sum_{m=1}^{N_c} w_m \cdot e^{-j\cdot\Omega_m\cdot k} = \frac{1}{\sqrt{N_c}} \sum_{m=1}^{N_c} A \cdot \sin\left(\omega_0 \cdot m \cdot \frac{T}{N_c}\right) \cdot e^{-j\cdot\Omega_m\cdot k} \\ &= \frac{A}{\sqrt{N_c}} \sum_{m=1}^{N_c} \frac{e^{\left\{j\cdot\omega_0\cdot m\cdot\frac{T}{N_c}\right\}} - e^{\left\{-j\cdot\omega_0\cdot m\cdot\frac{T}{N_c}\right\}}}{2j} \cdot e^{\left\{-j\cdot\frac{2\pi}{N_c}\cdot m\cdot k\right\}} \\ &= \frac{A}{2j\sqrt{N_c}} \sum_{m=1}^{N_c} \left[e^{jm\left\{\frac{\omega_0\cdot T - 2\pi\cdot k}{N_c}\right\}} - e^{-jm\left\{\frac{\omega_0\cdot T + 2\pi\cdot k}{N_c}\right\}}\right] \end{aligned} \tag{31}$$

The expressions (31) become straightforward if the frequency ω_0, the time T and the number of samples are related as

$$\omega_0 = \frac{2\pi}{N_0}, \qquad T = p \cdot N_0, \qquad N_c = p \cdot N_0,$$

where constants N_0 and p are all some natural numbers, $N_0,\, p \in \mathbb{N}$. In this case, Eqn. (31) takes the form

$$W_k = \frac{A}{2j\sqrt{N_c}} \sum_{m=1}^{N_c} \left[e^{j\cdot 2\pi\cdot m\cdot\frac{p-k}{N_c}} - e^{-j\cdot 2\pi\cdot m\cdot\frac{p+k}{N_c}}\right] \tag{32}$$

while, the sum in the right-hand side of the last formula can be readily found. Indeed, since

$$\sum_{m=1}^{N_c} e^{j\cdot 2\pi\cdot m\cdot\frac{n}{N_c}} = \begin{cases} N_c, & \text{if} \quad n = 0 \\ 0, & \text{if} \quad n = \pm 1,\, \pm 2,\, \ldots \end{cases}$$

then the amplitudes of W_k become

$$|W_k|^2 = \begin{cases} N_c \cdot \frac{A^2}{4}, & \text{if} \quad k = \pm p \mod N_c \\ 0, & \text{if} \quad k \neq \pm p \mod N_c \end{cases} \tag{33}$$

having a spike on the frequency of the continuous-in-time signal (29). ∎

The concept of the periodogram is closely linked to the notion of *spectrum* of an *infinite sequence* of samples of a signal if such a sequence would be available.

Definition 2 ([10]) Given an infinite sequence

$$\{w_k\}_{k=1}^{\infty} = \{w_1, w_2, \ldots, w_k, \ldots\},$$

originated from sampling a random signal $w(t)$ on a time interval $[0, +\infty)$ at time instances $t_k = \triangle \cdot k$, $k = 1, 2, \ldots$, i.e. $w_k := w(t_k)$ with the sampling period $\triangle$ (sec), this random sequence is said to be *quasi-stationary* if

$$\begin{array}{rclrcll} Ew_k & = & m_k, & |m_k| & \leq & C & \forall\, k \\ Ew_k w_l & = & R(k,l), & |R(k,l)| & \leq & C & \forall\, k,\, l \end{array} \tag{34}$$

and there exist limits

$$R_s(n) := \lim_{N\to\infty} \frac{1}{N} \sum_{m=1}^{N} R(m, m-n), \quad \forall\, n. \tag{35}$$

Here E denotes expectation of the stochastic components of $\{w_k\}_{k=1}^{\infty}$ or their functions. The *spectrum* of the quasi-stationary random sequence $\{w_k\}_{k=1}^{\infty}$ is then a complex-valued function

$$\Phi_s(\omega) := \sum_{n=-\infty}^{+\infty} R_s(n) e^{-j\cdot\omega\cdot n} \tag{36}$$

defined for those $\omega \in [0, 2\pi)$, where the sum is finite. ■

Loosely speaking, the spectrum $\Phi(\cdot)$ is defined as a Fourier transform of the *covariance function* $R_s(\cdot)$ keeping in mind that the term is only correct if $\{w_k\}_{k=1}^{\infty}$ is a stationary stochastic process with zero mean value. The usefulness of the presented concepts is in their abilities to handle and characterize both stochastic and deterministic signals as well as their linear combinations.

Example 2 The *finite* deterministic sequence (30) considered in Example 1 can be seen as a *truncated approximation* of the infinite one, and for which the rest of components is substituted by zeros, i.e.

$$\{w_k\}_{k=1}^{\infty} = \{A\sin(\omega_0\triangle\cdot 1), \ldots, A\sin(\omega_0\triangle\cdot k), \ldots, A\sin(\omega_0\triangle\cdot N_c), 0, 0, \ldots\}$$

Let us compute the spectrum of the *infinite* sequence derived from sampling the sinusoidal signal (29) every $\triangle$ (sec), i.e.

$$\{w_k\}_{k=1}^{\infty} = \{A\sin(\omega_0\triangle\cdot 1), \ldots, A\sin(\omega_0\triangle\cdot k), \ldots\} \tag{37}$$

Since the sequence is deterministic, then the values of m_k and $R(k,l)$ defined in Eqn. (34) are

$$m_k = A \cdot \sin\big(\omega_0 \triangle \cdot k\big), \quad R(k,l) = A^2 \cdot \sin\big(\omega_0 \triangle \cdot k\big) \cdot \sin\big(\omega_0 \triangle \cdot l\big)$$

and bounded as requested in (34). The direct computations show that

$$\begin{aligned}
\frac{1}{N}\sum_{m=1}^{N} R(m, m-n) = & \\
&= \frac{1}{N}\sum_{m=1}^{N} A^2 \cdot \sin\big(\omega_0 \triangle m\big) \cdot \sin\big(\omega_0 \triangle [m-n]\big) \\
&= \frac{A^2}{N}\sum_{m=1}^{N} \frac{e^{j\omega_0\triangle m} - e^{-j\omega_0\triangle m}}{2j} \cdot \frac{e^{j\omega_0\triangle [m-n]} - e^{-j\omega_0\triangle [m-n]}}{2j} \\
&= -\frac{A^2}{2N}\sum_{m=1}^{N} \left[\frac{e^{j\omega_0\triangle [2m-n]} + e^{-j\omega_0\triangle [2m-n]}}{2} - \frac{e^{j\omega_0\triangle n} + e^{-j\omega_0\triangle n}}{2}\right] \\
&= -\frac{A^2}{2N}\sum_{m=1}^{N} \Big[\cos\big(\omega_0\triangle [2m-n]\big) - \cos\big(\omega_0\triangle n\big)\Big] \\
&= -\frac{A^2}{2N}\sum_{m=1}^{N} \cos\big(\omega_0\triangle [2m-n]\big) + \frac{A^2}{2}\cos\big(\omega_0\triangle n\big)
\end{aligned}$$

If constants ω_0 and $\triangle$ are such that[3]

$$\lim_{N\to+\infty} \frac{1}{N}\sum_{m=1}^{N} \cos\big(\omega_0\triangle [2m-n]\big) = 0, \quad \forall\, n$$

then $R_s(n)$ is defined for any integer n and equals to

$$R_s(n) = \lim_{N\to+\infty} \frac{1}{N}\sum_{m=1}^{N} R(m, m-n) = \frac{A^2}{2}\cos\big(\omega_0 \cdot \triangle \cdot n\big). \tag{38}$$

Consequently, we can computer the Fourier transform of such *covariance*

[3]For instance, this is the case when $\omega_0 = \frac{2\pi}{N_0}$ for some $N_0 \in \mathbb{N}$ and $\triangle = 1$ (*sec*).

function and obtain the spectrum of the infinite sequence (37) as

$$\begin{aligned}\Phi(\omega) &= \sum_{n=-\infty}^{+\infty} \frac{A^2}{2} \cos\big(\omega_0 \cdot \triangle \cdot n\big) \cdot e^{-j\cdot\omega\cdot n} \\ &= \frac{A^2}{2} \sum_{n=-\infty}^{+\infty} \frac{e^{j\omega_0\cdot\triangle\cdot n} + e^{-j\omega_0\cdot\triangle\cdot n}}{2} \cdot e^{-j\cdot\omega\cdot n} \\ &= \frac{A^2}{4} \sum_{n=-\infty}^{+\infty} \Big[e^{j(\omega_0\cdot\triangle-\omega)\cdot n} + e^{-j(\omega_0\cdot\triangle+\omega)\cdot n}\Big] \\ &= \frac{A^2}{4}\Big[\delta(\omega_0\cdot\triangle-\omega) + \delta(\omega_0\cdot\triangle+\omega)\Big] \end{aligned} \tag{39}$$

and where $\delta(\cdot)$ is the Dirac delta function (known as well as the unit impulse) applied at 0. Comparing the formula for the periodogram (33) computed for the truncated sequence and the formula (39) for the spectrum of the sinusoidal wave sampled with time step of $\triangle = 1$ (sec), one can observe the link between two concepts and the explicit format of the approximation of the spectrum by the periodogram. ■

The next concept, which is important for the study and which naturally appears in processing sampled measurements of the continuous-in-time signals $\theta(\cdot)$ and $v(\cdot)$, is a linear *discrete-in-time* model

$$\begin{aligned}&\tilde{a}_n y_{k+n} + \tilde{a}_{n-1} y_{k+n-1} + \ldots + \tilde{a}_1 y_{k+1} + \tilde{a}_0 y_k \\ &\qquad = \tilde{b}_l u_{k+l} + \tilde{b}_{l-1} u_{k+l-1} + \cdots + \tilde{b}_1 u_{k+1} + \tilde{b}_0 u_k \end{aligned} \tag{40}$$

with

$$y_k := y(t)|_{t=k\cdot\triangle}\,, \qquad u_k := u(t)|_{t=k\cdot\triangle} \tag{41}$$

and the corresponding *discrete-time* transfer function

$$G_q(z) := \frac{\tilde{b}_l z^l + \tilde{b}_{l-1} z^{l-1} + \cdots + \tilde{b}_1 z + \tilde{b}_0}{\tilde{a}_n z^n + \tilde{a}_{n-1} z^{n-1} + \cdots + \tilde{a}_1 z + \tilde{a}_0}. \tag{42}$$

As known, it relates the so-called z-transforms of the sampled sequences of the continuous-in-time signals for the given transfer function $G(s)$ of the linearized continuous-in-time dynamics (13) defined next.

Definition 3 Given an infinite sequence $\big\{w_k\big\}_{k=-\infty}^{k=+\infty}$ of real numbers, the following complex-valued function of complex variable

$$W(z) := \sum_{k=-\infty}^{+\infty} w_k z^{-k} \tag{43}$$

is referred to as its *z-transform* provided that the series values are defined (finite) for some open subset of complex plane. ■

According to the following statement [5, p. 337], sampled continuous-in-time solutions (41) of the linear control system are indeed solutions of a discrete-in-time linear control system (40).

Lemma 3 *Given a solution of* $\big[y(t), u(t)\big]$ *of a linear continuous-in-time control system (10) with* $y(\tau) = u(\tau) \equiv 0$, $\forall\, \tau < 0$, *consider infinite sequences* $\big\{y_k\big\}_{k=-\infty}^{k=+\infty}$, $\big\{u_k\big\}_{k=-\infty}^{k=+\infty}$ *created by sampling the solution with the period* $\triangle$, *see (41), then these sequences are a solution of the linear discrete-in-time system (40) with the transfer function (42)*

$$G_q(z) = \frac{z-1}{z} \cdot \mathcal{Z}\Big(\textit{sampled step response of } G(s)\Big) \tag{44}$$

where $G(s)$ *is the transfer function (12) of the linear control system (10) and* $\mathcal{Z}(\cdot)$ *is the z-transform of the argument.* ■

The immediate consequence of the statement for the grey-box model (5) of the case study with the linearization about the stable equilibrium (8) is the following

Lemma 4 *Given the linearization (8) of the grey-box model (5) about its stable equilibrium at* $\theta_e = 0$, *suppose the parameters* p_1-p_4 *satisfy the constraint*[4]

$$0 < \frac{p_2}{2\sqrt{p_1 p_3}} < 1, \tag{45}$$

consider a solution $\big[y(t), u(t)\big]$ *of (8) with* $y(\tau) = u(\tau) \equiv 0$, $\forall\, \tau < 0$ *and introduce infinite sequences* $\big\{y_k\big\}_{k=-\infty}^{k=+\infty}$, $\big\{u_k\big\}_{k=-\infty}^{k=+\infty}$ *obtained by sampling the solution with the period* $\triangle$ *(sec), then these sequences are a solution of the linear discrete-in-time system*

$$y_{k+2} + \tilde{a}_1 y_{k+1} + \tilde{a}_0 y_k = \tilde{b}_1 u_{k+1} + \tilde{b}_0 u_k \tag{46}$$

[4]That assumption is linked to the model of viscous friction for the system, and, as observed further in the text, it is in place for the case study.

with coefficients

$$\tilde{a}_0 = e^{-2\cdot\triangle\cdot\psi\cdot\omega_n}, \tag{47}$$

$$\tilde{a}_1 = -2\cdot e^{-\triangle\cdot\psi\cdot\omega_n}\cdot\cos\left(\triangle\cdot\omega_n\cdot\sqrt{1-\psi^2}\right), \tag{48}$$

$$\tilde{b}_0 = \gamma\cdot\left[e^{-2\cdot\triangle\cdot\psi\cdot\omega_n}+\frac{e^{-\triangle\cdot\psi\cdot\omega_n}}{\sqrt{1-\psi^2}}\sin\left(\triangle\cdot\omega_n\cdot\sqrt{1-\psi^2}-\beta\right)\right], \tag{49}$$

$$\tilde{b}_1 = \gamma\cdot\left[1-\frac{e^{-\triangle\cdot\psi\cdot\omega_n}}{\sqrt{1-\psi^2}}\sin\left(\triangle\cdot\omega_n\cdot\sqrt{1-\psi^2}+\beta\right)\right]. \tag{50}$$

Here the parameters

$$\psi := \frac{p_2}{2\sqrt{p_1 p_3}}, \quad \omega_n := \sqrt{\frac{p_3}{p_1}}, \quad \gamma := \frac{p_4}{p_3}, \tag{51}$$

are constants defined by p_1-p_4*, and* β *is an angle,* $0<\beta<\frac{\pi}{2}$*, such that*

$$\cos\beta = \psi \qquad \big(\textit{and therefore} \quad \sin\beta = \sqrt{1-\psi^2}\big), \tag{52}$$

all used for brevity of the expressions in (47)-(50). ■

Proof: To start with, let us derive the discrete-in-time linear system for a specific version of the linear system (8), namely, when the positive parameters p_1-p_4 are such that the continuous-in-time dynamics can be re-written as follows

$$\tfrac{d^2}{dt^2}y(t)+2\cdot\psi\cdot\omega_n\cdot\tfrac{d}{dt}y(t)+\omega_n^2\cdot y(t)=\omega_n^2\cdot u(t). \tag{53}$$

Its transfer function takes the form

$$G(s)=\frac{\omega_n^2}{s^2+2\cdot\psi\cdot\omega_n\cdot s+\omega_n^2},$$

and, according to the formula (44) of Lemma 3, the discrete-in-time linear control system, which a $\triangle$-sampled solution of (53) satisfies, has the following

transfer function

$$
\begin{aligned}
G_q(z) \;=\; & \frac{z-1}{z}\cdot\mathcal{Z}\Big(\text{sampled step response of } G(s)\Big) \\
=\; & \frac{z-1}{z}\cdot\mathcal{Z}\left(\left[1-\frac{e^{-t\cdot\psi\cdot\omega_n}}{\sqrt{1-\psi^2}}\sin\Big(t\cdot\omega_n\sqrt{1-\psi^2}+\beta\Big)\right]\Big|_{t=k\cdot\triangle,k=0,1,\ldots}\right) \\
=\; & \frac{z-1}{z}\cdot\mathcal{Z}\Big(\big[\,1\,\big]\big|_{t=k\triangle,\,k=0,1,\ldots}\Big) \\
& -\frac{z-1}{z}\cdot\mathcal{Z}\left(\left[\frac{e^{-t\cdot\psi\cdot\omega_n}}{\sqrt{1-\psi^2}}\cdot\sin\Big(t\cdot\omega_n\sqrt{1-\psi^2}\Big)\cdot\cos(\beta)\right]\Big|_{t=k\cdot\triangle,k=0,1,\ldots}\right) \\
& -\frac{z-1}{z}\cdot\mathcal{Z}\left(\left[\frac{e^{-t\cdot\psi\cdot\omega_n}}{\sqrt{1-\psi^2}}\cdot\cos\Big(t\cdot\omega_n\sqrt{1-\psi^2}\Big)\cdot\sin(\beta)\right]\Big|_{t=k\cdot\triangle,k=0,1,\ldots}\right) \\
=\; & \frac{z-1}{z}\cdot\mathcal{Z}\Big(\big[\,1\,\big]\big|_{k=0,1,\ldots}\Big) \qquad (54)\\
& -\frac{z-1}{z}\cdot\frac{\cos(\beta)}{\sqrt{1-\psi^2}}\cdot\mathcal{Z}\left(\Big[e^{(-\triangle\psi\omega_n)\cdot k}\cdot\sin\big((\triangle\omega_n\sqrt{1-\psi^2})\cdot k\big)\Big]\Big|_{k=0,1,\ldots}\right) \\
& -\frac{z-1}{z}\cdot\frac{\sin(\beta)}{\sqrt{1-\psi^2}}\cdot\mathcal{Z}\left(\Big[e^{(-\triangle\psi\omega_n)\cdot k}\cdot\cos\big((\triangle\omega_n\sqrt{1-\psi^2})\cdot k\big)\Big]\Big|_{k=0,1,\ldots}\right)
\end{aligned}
$$

As known [5, p. 323], the z-transforms of the signals

$$\mathcal{Z}\Big(\big[\,1\,\big]\big|_{k=0,1,\ldots}\Big) \;=\; \frac{z}{z-1} \qquad (55)$$

$$\mathcal{Z}\Big(\big[a^k\cdot\sin\big(\phi\cdot k\big)\big]\big|_{k=0,1,\ldots}\Big) \;=\; \frac{\big(a\sin\phi\big)\cdot z}{z^2-2\cdot\big(a\cos\phi\big)\cdot z+a^2} \qquad (56)$$

$$\mathcal{Z}\Big(\big[a^k\cdot\cos\big(\phi\cdot k\big)\big]\big|_{k=0,1,\ldots}\Big) \;=\; \frac{\big(z-a\cos\phi\big)\cdot z}{z^2-2\cdot\big(a\cos\phi\big)\cdot z+a^2} \qquad (57)$$

Therefore, denoting

$$a := e^{-\triangle\cdot\psi\cdot\omega_n},\quad \phi := \triangle\cdot\omega_n\cdot\sqrt{1-\psi^2},$$

one can continue (54) as

$$
\begin{aligned}
G_q(z) \;=\; & \frac{z-1}{z}\cdot \underbrace{\frac{z}{z-1}}_{\text{see (55)}} \;-\frac{z-1}{z}\cdot\frac{\overbrace{\psi}^{\text{see (52)}}}{\sqrt{1-\psi^2}}\cdot\underbrace{\frac{\big(a\sin\phi\big)\cdot z}{z^2-2\cdot\big(a\cos\phi\big)\cdot z+a^2}}_{\text{see (56)}} \\
& \qquad -\frac{z-1}{z}\cdot\frac{\overbrace{\sqrt{1-\psi^2}}^{\text{see (52)}}}{\sqrt{1-\psi^2}}\cdot\underbrace{\frac{\big(z-a\cos\phi\big)\cdot z}{z^2-2\cdot\big(a\cos\phi\big)\cdot z+a^2}}_{\text{see (57)}} \\
= \;& 1-\frac{\psi}{\sqrt{1-\psi^2}}\cdot\frac{\big(a\sin\phi\big)\cdot(z-1)}{z^2-2\cdot\big(a\cos\phi\big)\cdot z+a^2} \\
& \qquad -\frac{\big(z-a\cos\phi\big)\cdot(z-1)}{z^2-2\cdot\big(a\cos\phi\big)\cdot z+a^2} \\
= \;& \frac{z\cdot\Big(1-\frac{a}{\sqrt{1-\psi^2}}\big(\sqrt{1-\psi^2}\cos\phi+\psi\sin\phi\big)\Big)}{z^2-2\cdot\big(a\cos\phi\big)\cdot z+a^2} \\
& \qquad +\frac{a\cdot\Big(a+\frac{1}{\sqrt{1-\psi^2}}\big(\psi\cdot\sin\phi-\sqrt{1-\psi^2}\cdot\cos\phi\big)\Big)}{z^2-2\cdot\big(a\cos\phi\big)\cdot z+a^2} \\
= \;& \frac{z\cdot\Big(1-\frac{a}{\sqrt{1-\psi^2}}\sin\big(\phi+\beta\big)\Big)+a\cdot\Big(a+\frac{1}{\sqrt{1-\psi^2}}\sin\big(\phi-\beta\big)\Big)}{z^2-2\cdot\big(a\cos\phi\big)\cdot z+a^2}
\end{aligned}
\tag{58}
$$

To take advantage of the derived format of the discretization (58) for the particular linear continuous-in-time system (53) and to proceed with computing the discretization for the general format of the system (8), one can observe that the difference of the continuous-in-time systems is in the gain of the control input. So that re-scaling the input by the constant factor γ to meet the identity

$$
\omega_n^2\cdot\big(\gamma\cdot u(t)\big) \;\equiv\; \frac{p_4}{p_1}\cdot u(t), \qquad \forall\, t
$$

results in its value as mentioned in (51) and adjusts accordingly the coefficients of the right-hand side of the difference equation (46). ■

Transformation of periodograms by stable linear discrete-in-time systems admits the following characterization, see [10, p. 31]

Theorem 1 *Let infinite sequences* $\{y_k\}_{k=-\infty}^{k=+\infty}$, $\{u_k\}_{k=-\infty}^{k=+\infty}$ *of real numbers be related by the stable linear system*[5] *(40), suppose the input sequence* $\{u_k\}_{k=-\infty}^{k=+\infty}$ *is unknown for* $k \leq 0$, *but obeys* $|u_k| < C_u$ *for all* k. *Let*

$$Y_N(\omega) = \frac{1}{\sqrt{N}} \sum_{k=1}^{N} y_k e^{-j\omega k}, \qquad U_N(\omega) = \frac{1}{\sqrt{N}} \sum_{k=1}^{N} u_k e^{-j\omega k}, \tag{59}$$

then

$$Y_N(\omega) = G_q\big(e^{j\omega}\big) U_N(\omega) + R_N(\omega) \tag{60}$$

with

$$\big|R(\omega)\big| \leq \frac{C}{\sqrt{N}}$$

where the constant C *is independent of* N. ■

This and all the modelling and analysis arguments above form the basis for

---

Identification procedure:

Step 1: Choose an amplitude A and a frequency ω_0 of the sinusoidal input and record the system response

Step 2: Resample the data and compute periodograms

Step 3: Compute estimate for $G_q\big(e^{j\omega_0}\big)$ taking advantage of (60)

Step 4: Use intermediate estimates $\widehat{G}_q\big(e^{j\omega_k}\big)$ repeatedly computed following **Steps 1-3** for several frequencies $\{\omega_k\}$ for deriving estimates for the parameters p_1-p_4 or their functions

---

The listed steps are first implemented for analysis of synthetic data generated by simulation of forced responses of nonlinear control system in a vicinity of its stable equilibrium. In the next Section they are repeated for processing experimental data.

[5]The linear system (40) is stable if all the roots of the polynomial equation

$$\tilde{a}_n z^n + \tilde{a}_{n-1} z^{n-1} + \cdots + \tilde{a}_1 z + \tilde{a}_0 = 0$$

have their amplitudes less than 1.

2.3 Estimates of parameters for synthetic model

As a preliminary example for analysis, we have considered the nonlinear dynamic system (2) with the following values of mechanical sub-part

$$m_p = 0.1\ [kg], \quad l_c = 0.05\ [m], \quad J_p = 0.003\ [Nm], \quad g = 9.81\ [m/s^2] \tag{61}$$

and some reasonable choices of parameters of the electrical sub-system that altogether resulted in the following parameters of the grey-box model (5)

$$p_1 = 0.00325, \quad p_2 = 0.001, \quad p_3 = 0.04905, \quad p_4 = 10. \tag{62}$$

The linearization (10) of such nonlinear grey-box model of the system about its downward equilibrium $\theta_e = 0$ has the next transfer function

$$G(s) = \frac{b_0}{s^2 + a_1 s + a_0}, \quad a_1 \approx 0.308, \quad a_0 \approx 15.09, \quad b_0 \approx 3076.9. \tag{63}$$

2.3.1 Step 1: Choose the ranges of amplitudes and frequencies of input and record responses

Since the system (5) is nonlinear and of substantial amplification of the control input – at least of

$$\gamma = \frac{p_4}{p_3} \approx 200$$

for steady-state values, – then the choice of input amplitudes and frequencies should be taken with care to make the responses of linearization be somehow close to responses of nonlinear system. The natural frequency ω_n of the linearized system and its damping ratio ψ, see (51), are equal to

$$\psi := \frac{p_2}{2\sqrt{p_1 p_3}} \approx 0.04, \qquad \omega_n = \sqrt{\frac{p_3}{p_1}} \approx 3.88$$

and correspond to stable lightly damped linear control system of second order. This suggests the choices of frequencies of input signal

$$\big[1,\ 1.5,\ 2,\ 2.5,\ 3,\ 3.5,\ 4,\ 4.5,\ 5,\ 5.5,\ 6,\ 6.5,\ 7\big] \tag{64}$$

equally spread about the natural frequency $\omega_n \approx 3.88\ \left(\frac{rad}{sec}\right)$ of the linearized dynamics. The amplitudes of input sin-waves have been chosen small enough to keep forced oscillations of the nonlinear system (5) in the range of $\pm 10^\circ$ from the downward equilibrium $\theta_e = 0$.

The non-linear model of the system (5) has been built in Simulink. The simulations has run for substantial time interval to observe the forced steady-state oscillations in response. Couple of such responses are depicted on Figs. 3 and 4, where one can observe the transition and the steady-state oscillations of the nonlinear system forced by input sin-waves. As mentioned above, amplitudes of that oscillations play the key role in identification procedure.

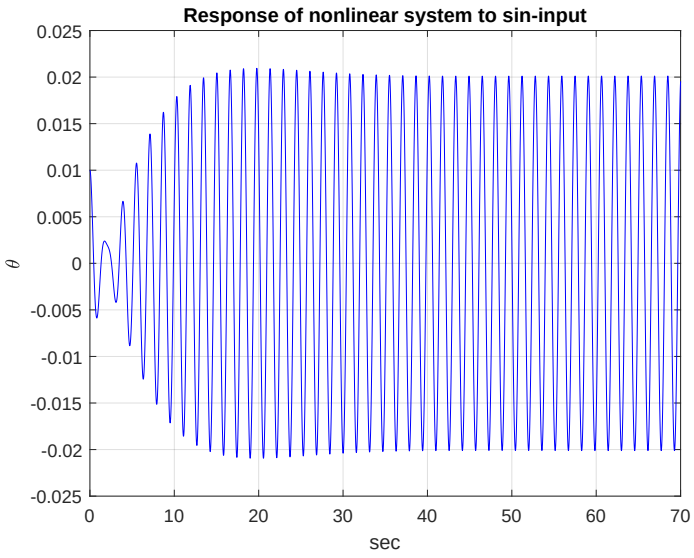

Figure 3: The time response of the system (5) with the parameters (62) to the input $v(t) = A \cdot \sin\big(\omega \cdot t\big)$ with $\omega = 4$ $[rad/sec]$ and $A = 10^{-5}$.

2.3.2 Step 2: Process the data and obtain the periodograms of signals

The simulated responses of the grey-box model (5) has been intentionally obtained with high accuracy and small step-size by the `ode45`-solver. Prior computing the DFT of the signals $v(\cdot)$ and $\theta(\cdot)$, they have been equidistantly down-sampled to

$$\triangle = 0.04 \ (sec).$$

The results for one of the responses is depicted on Fig. 5. According to Lemma 4, the transfer function $G_q(z)$ of the discrete-in-time linear control system (46) defined for the nominal model (63) for the sampling period 0.04 (sec) takes the form

$$G_q(z) = \frac{\tilde{b}_1 z + \tilde{b}_0}{z^2 + \tilde{a}_1 z + \tilde{a}_0}, \tag{65}$$

with

$$\tilde{a}_1 \approx -1.9638, \quad \tilde{a}_0 \approx 0.9878, \quad \tilde{b}_1 \approx 2.4465, \quad \tilde{b}_0 \approx 2.4365 \tag{66}$$

The periodograms of the DFT of the resampled responses of the system for the its (almost) steady-state behavior taken for the last 40 (sec) of the resampled data (25) have been computed based on Eqns. (27)-(28). As discussed in Example 1, the periodogram of a pure sin-wave input $v(\cdot)$ will have

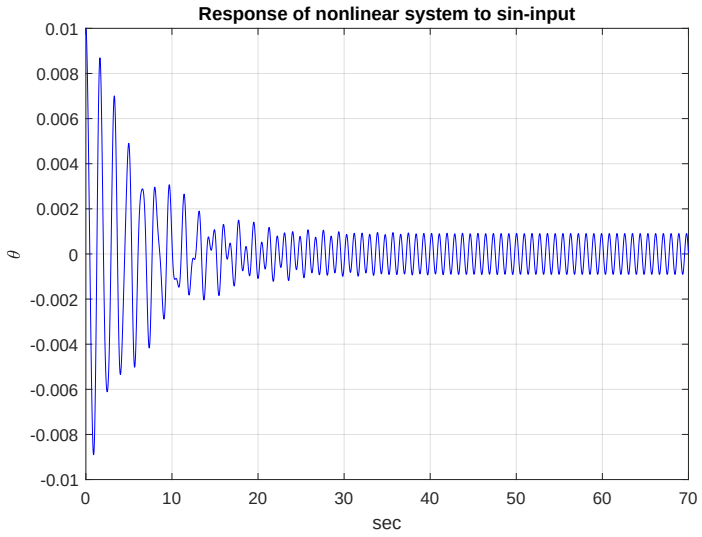

Figure 4: The time response of the system (5) with the parameters (62) to the input $v(t) = A \cdot \sin\big(\omega \cdot t\big)$ with $\omega = 7$ $[rad/sec]$ and $A = 10^{-5}$.

non-zero peak close to the its frequency. Meanwhile the periodogram of the response $\theta(\cdot)$ of the nonlinear system (5) might be more complex, and the repetitive (cyclic) behavior observed on Fig. 5 and the like, is, in fact, a sine-wave in approximation. In supporting the point, it is worth to examine the periodogram of the resampled response depicted on Fig. 6, where one can observe minor but non-negligible peaks in a vicinity of the dominant input sin-wave frequency of 4 $\big(rad/sec\big)$.

2.3.3 Step 3: Compute estimate for $G_q\big(z\big)$

Having computed the DFTs for the resampled sequences $\big\{\theta_k\big\}_{k=1}^{k=N}$, $\big\{v_k\big\}_{k=1}^{k=N}$ and denoted as $\Theta_N(\cdot)$ and $V_N(\cdot)$, we can take advantage the relation (60) and provide various estimates for the transfer function of the discrete-in-time model at particular arguments. Indeed, since the corresponding solutions $\theta(\cdot)$ and $y(\cdot)$ of the nonlinear and linear systems (5) and (8) for the same sinusoidal inputs are close, then the periodograms of such functions should be close as well

$$\Theta_N(\omega) \approx Y_N(\omega) \tag{67}$$

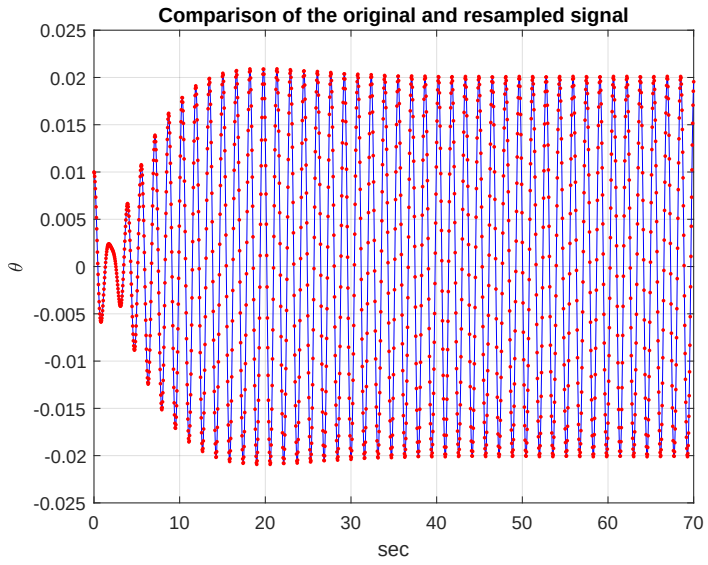

Figure 5: The time response of the system (5) with the parameters (62) to the input $v(t) = A \cdot \sin\big(\omega \cdot t\big)$ with $\omega = 4$ $[rad/sec]$ and $A = 10^{-5}$ depicted in blue versus its down-sampled representation of 0.04 (sec) step-size shown by red dots.

at least for some range of frequencies. Furthermore, the relation (60) for large N implies that

$$\frac{\big|Y_N(\omega)\big|}{\big|U_N(\omega)\big|} \approx \big|G_q\big(e^{j\omega}\big)\big|$$

and the fraction on the left can be used as asymptotically unbiased estimator for the value on the right-hand side. Therefore, for those frequencies, where the approximation (67) holds, we obtain

$$\boxed{\frac{\big|\Theta_N(\omega)\big|}{\big|V_N(\omega)\big|} \approx \big|G_q\big(e^{j\omega}\big)\big|} \tag{68}$$

The formula (68) can be seen a starting point for reconstruction of $G_q(z)$. Indeed, the left-hand side of (68) can be readily computed for those frequencies ω, where the response of the nonlinear system (5) to an input sin-wave is close to a sine-wave itself. For this case, the periodograms of $\big\{\theta_k\big\}_{k=1}^{k=N}$ and $\big\{v_k\big\}_{k=1}^{k=N}$ will have only one dominant peak at the frequency of the sinusoidal signal, and, as discussed in Example 1, the fraction (68) equals to

the relation of amplitudes of sines at the input and at the output

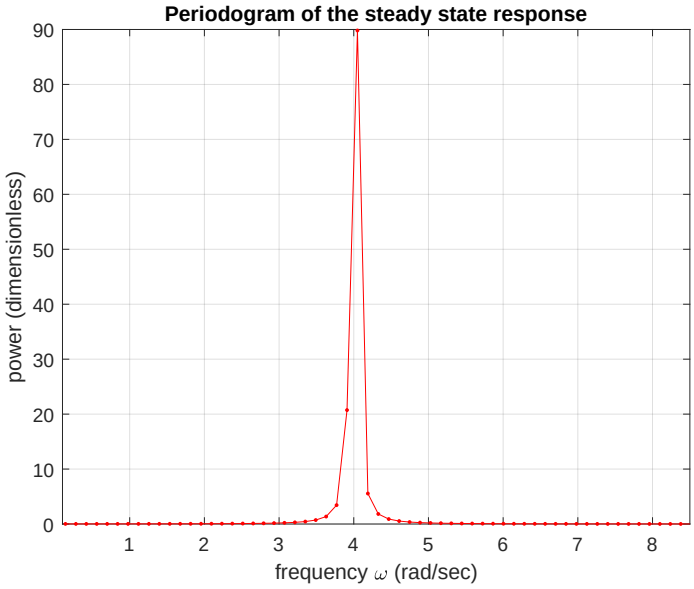

Figure 6: The periodogram of the resampled (steady-state) response of the nonlinear system (5) to the sin-wave of frequency 4 $\big(rad/sec\big)$ that can be observed on Fig. 5 for the last 40 (sec). In contrast to response of a linear system, the response indeed differs from the scaled sin-wave of the same frequency. There are several non-negligible peaks on the graph suggesting that the oscillations are decomposed into a sum of sinusoidal signals of different frequencies even though the frequency of 4 $\big(rad/sec\big)$ is clearly dominant.

The next technical statement provides one of many estimators for an amplitude of almost sinusoidal signal.

Lemma 5 *Let $w(\cdot)$ be a bounded function of the form*

$$w(t) = A \cdot \sin\big(\omega \cdot t\big) + \varepsilon(t) \tag{69}$$

with A and ω being positive constants and $\varepsilon(\cdot)$ being a function such that

$$\lim_{T\to+\infty} \frac{1}{T} \int_0^T \sin\big(\omega t\big) \cdot \varepsilon(t) dt = \lim_{T\to+\infty} \frac{1}{T} \int_0^T \varepsilon^2(t) dt = 0, \tag{70}$$

then

$$A = \lim_{T\to+\infty} \sqrt{\frac{2 \cdot S(T)}{T}}, \tag{71}$$

where $S(T)$ is any positive function such that

$$\lim_{T\to+\infty} \frac{S(T)}{\int_0^T w^2(t) dt} = 1.$$

Proof of Lemma comes from straightforward observation that

$$\begin{aligned}\int_0^T w^2(t)dt &= \int_0^T \left\{A\cdot\sin\big(\omega t\big)+\varepsilon(t)\right\}^2 dt \\ &= A^2\int_0^T \sin^2\big(\omega t\big)dt + 2A\int_0^T \sin\big(\omega t\big)\cdot\varepsilon(t)dt + \int_0^T \varepsilon^2(t)dt \\ &= A^2\left[\frac{T}{2}-\frac{\sin\big(2T\big)}{4}\right] + 2A\int_0^T \sin\big(\omega t\big)\cdot\varepsilon(t)dt + \int_0^T \varepsilon^2(t)dt.\end{aligned}$$

If we divide both sides of the last equation on T and pass to limit when T goes to $+\infty$, then we obtain in the right-hand side

$$\begin{aligned}\lim_{T\to+\infty}\frac{1}{T}\left\{A^2\left[\frac{T}{2}-\frac{\sin\big(2T\big)}{4}\right] + 2A\int_0^T \sin\big(\omega t\big)\cdot\varepsilon(t)dt + \int_0^T \varepsilon^2(t)dt\right\} \\ = A^2\lim_{T\to+\infty}\frac{1}{T}\left[\frac{T}{2}-\frac{\sin\big(2T\big)}{4}\right] = \frac{1}{2}A^2.\end{aligned}$$

Here we have used the relations (70) to null the second and third summands when computed passed to limit. Meanwhile, the left-hand side takes the form

$$\begin{aligned}\lim_{T\to+\infty}\frac{1}{T}\int_0^T w^2(t)dt &= \lim_{T\to+\infty}\frac{\int_0^T w^2(t)dt}{T}\cdot\overbrace{\lim_{T\to+\infty}\frac{S(T)}{\int_0^T w^2(t)dt}}^{=1} \\ &= \lim_{T\to+\infty}\left[\frac{\int_0^T w^2(t)dt}{T}\cdot\frac{S(T)}{\int_0^T w^2(t)dt}\right] = \lim_{T\to+\infty}\frac{S(T)}{T},\end{aligned}$$

where we have taken an advantages of the property of the function $S(\cdot)$ mentioned in Lemma. Comparing now both sides we obtain an equivalent expression to the limit relation (71). ∎

Remark 5 Obviously, there are alternative methods for estimating an amplitude of a sin-wave (69) from noisy and sampled observations. One can think of searching local maximal (minimal) values of (69) and averaging them; or fitting data on slopes of sine-waves *ect.* Meanwhile, processing experimental data show that the formula (71) gives often robust results when

the function $S(\cdot)$ is chosen as a numerical quadrature of squared centered measured signal. In this respect, computing robustly the mean-value (and de-trending) of measurements becomes also interesting question, but we postpone it to the next Section. ■

The results for the set of input sin-waves with frequencies (64) for individual realizations for each frequency, where the estimates (68) have been computed based on the formula (71), are shown on Fig. 7. The values depicted as red crosses **"x"** correspond to the results of analysis of data obtained for the scenario when the measured response of the nonlinear system (5) contains no noise. They reproduce closely the Bode plot of a lightly damped linear second order system (63) with resonance peak located somewhere on the interval $[3.75, 4]$ $\left(\frac{rad}{sec}\right)$. The values depicted as blue circles **"o"** correspond to the results of analysis of the response of the nonlinear (5) spoiled by noise of some energy. The plot is far from a detailed reconstruction of the Bode plot of the linear system, while the resonance peak is well recovered on the same interval of frequencies.

2.3.4 Step 4: Deriving estimates for the parameters p_1-p_4 or their functions

As seen on Fig. 7, the profile of response can be substantially dependent on a noise or non-modelled non-linearity (such as dry friction, hysteresis in crossing zero velocity by a link *etc.*) unavoidable in robotic applications. Therefore, analysis and calibration of parameters of the nonlinear system (5) based on properties of its linearization (8) should be taken with care.

In this respect, it is worth to mention the standard practice of searching conditions for detecting (induced) oscillatory behaviours in dynamical systems and identification of parameters of a feedback controller or the system itself as functions of characteristics of such oscillations, see references [11, 5] and many others. Similar supporting arguments can be learned from Figs. 7 and 8, where despite measurement noise and non-linearity of the system dynamics the frequency of the resonance peak of the linearization is well reproduced. On Fig. 8, we have depicted the Bode plot of the linearization (8) of the nonlinear system (5) and superimposed by already presented estimates for amplitudes of amplification of input sine-waves passed through the nonlinear system, see Fig. 7. They are clearly in good match!

Therefore, we can expect that the frequency of such resonant (maximal in amplitude) oscillation is one of characteristics of the nonlinear system that is robust to the noise and some of non-modeled dynamics. For the linearization (63) that frequency can be found as follows

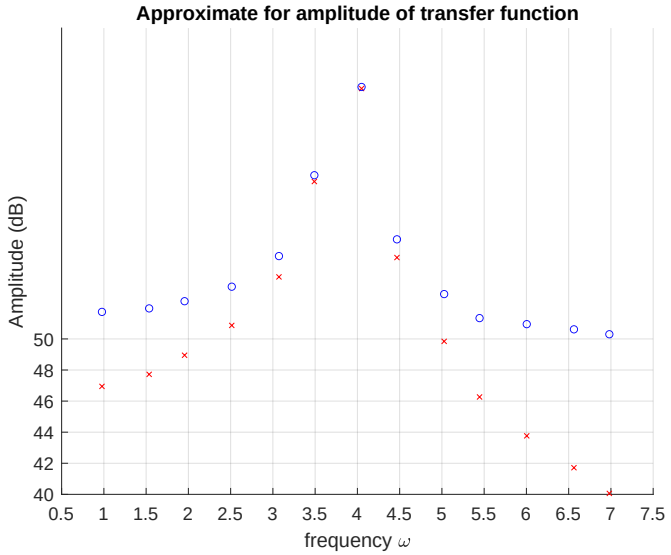

Figure 7: Estimates for the amplitude of the transfer function $G_q\big(e^{j\omega}\big)$ computed for the synthetic data based on the formula (68) and an asymptotic estimator (71) found for the range of frequencies (64). The values depicted as red crosses **"x"** correspond to the results of analysis of data obtained for the scenario when the measured response of the nonlinear system (5) contains no noise. They reproduce closely the Bode plot of a lightly damped linear second order system (63) with resonance peak on the interval $[3.5, 4]$ $\big(\frac{rad}{sec}\big)$. The values depicted as blue circles **"o"** correspond to the results of analysis of the response of (5) spoiled by noise of some energy. The plot is far from detailed reconstruction of the Bode plot of the linear system, while the resonance peak is well recovered on the same interval of frequencies.

Lemma 6 *Given the transfer function*

$$G(s) = \frac{b_0}{s^2 + a_1 \cdot s + a_0}, \qquad b_0 > 0,\ a_1 > 0,\ a_0 > 0 \tag{72}$$

a continuous-in-time second order linear control system (10), if $\big(a_0 - \frac{a_1^2}{2}\big) \geq 0$, *then the frequency*

$$\omega_{opt} := \sqrt{a_0 - \frac{a_1^2}{2}} \tag{73}$$

represents the argument, where the magnitude of the frequency response function $G\big(j\omega\big)$ *reaches its maximal value*

$$\big|G\big(j\omega_{opt}\big)\big| = \sup_{0 \leq \omega < +\infty} \big|G\big(j\omega\big)\big|$$

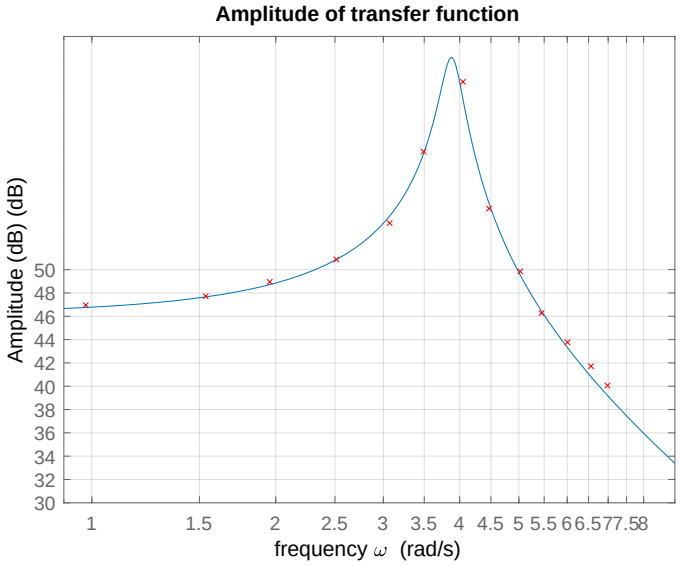

Figure 8: The **blue curve** is the amplitude Bode plot of the linearization (63) of the nonlinear system (5) when p_1-p_4 parameters have values (62); the red crosses **"x"** correspond to the results of analysis of data obtained through simulation of the nonlinear system (5) when its responses contains no measurement noise and the model (5) has no other contributions to the dynamics.

Otherwise, if $\left(a_0 - \frac{a_1^2}{2}\right) < 0$, *then* $\omega_{opt} = 0$. ■

Proof: The argument of maximum of the magnitude of the function $G\big(j\omega\big)$ is independent of the factor b_0, so that let us assume that $b_0 = 1$. Then

$$\begin{aligned} G\big(j\omega\big) &= \frac{1}{\big(j\omega\big)^2 + a_1 j\omega + a_0} = \frac{1}{\big(a_0 - \omega^2\big) + j a_1 \omega} \cdot \frac{\big(a_0 - \omega^2\big) - j a_1 \omega}{\big(a_0 - \omega^2\big) - j a_1 \omega} \\ &= \frac{a_0 - \omega^2}{\big(a_0 - \omega^2\big)^2 + a_1^2 \omega^2} - j \frac{a_1 \omega}{\big(a_0 - \omega^2\big)^2 + a_1^2 \omega^2}, \end{aligned}$$

where the summands represent the real and imaginary parts of the frequency response function. Therefore, the magnitude of $G\big(j\omega\big)$ is equal to

$$\big|G\big(j\omega\big)\big|^2 = \frac{1}{\big(a_0 - \omega^2\big)^2 + a_1^2 \omega^2}. \tag{74}$$

Denoting $x := \omega^2$ and

$$F(x) := \big|G\big(j\omega\big)\big|^2\Big|_{x=\omega^2} = \frac{1}{\big(a_0 - x\big)^2 + a_1^2 x}, \tag{75}$$

we search for point of maximal of $F(\cdot)$. As seen, it is inverse of a parabola which graph is always above zero level. Therefore, $F(\cdot)$ has only one global maximum (such parabola has one minimum!), which we can find by searching a critical point of $F(x)$, i.e. solving the equation

$$0 = \frac{d}{dx}F(x) = -\frac{2x - 2a_0 + a_1^2}{\left[\left(a_0 - x\right)^2 + a_1^2 x\right]^2}.$$

Clearly, the solution of the last equation is

$$x_{opt} = a_0 - \frac{a_1^2}{2}. \tag{76}$$

If it is positive, then the argument of maximum of the amplitude of the frequency response function is equal to a square root of that number. Otherwise, since, for the optimization problem $x = \omega^2$ and cannot be negative, then the argument of maximum is on the boundary of $x \in [0, +\infty)$. Clearly at $x = 0$ is positive, while at $x = +\infty$ is zero. So that the argument of maximum is zero. ■

Taking into account the relations (13)-(14) established in-between the coefficients of the transfer function $G(s)$ and parameters p_1-p_4 – or even physical parameters of the system with the help of (6), – the formula (73) becomes of the form

$$\omega_{opt} = \sqrt{\frac{p_3}{p_1} - \frac{1}{2}\left(\frac{p_2}{p_1}\right)^2} = \sqrt{\frac{m_p g l_c}{J_p + m_p l_c^2} - \frac{1}{2}\frac{\left(k_f + k_{emf}\cdot\frac{k_i}{R}\right)^2}{\left(J_p + m_p l_c^2\right)^2}} \tag{77}$$

As mentioned, the left-hand side of (77) can be estimated from the data and analysis of corresponding periodograms despite presence of moderate noise and non-linearities of the dynamics.

To take advantage of (77), one can propose to run a series of experiments with the so-called added mass of known quantity m_a attached to the system on given distance l_a from the axis of rotation. With such physical modification of the robotic system, the dynamics of its grey-box model (5) will be accordingly changed to new nonlinear system

$$\left(p_1 + m_a l_a^2\right)\cdot\ddot{\theta}(t) + p_2\cdot\dot{\theta}(t) + \left(p_3 + m_a g l_a\right)\cdot\sin\left(\theta(t)\right) = p_4\cdot v(t) + \tau_\varepsilon(t) \tag{78}$$

And the formula (77) will result in the expression

$$\omega_{opt} = \sqrt{\frac{p_3 + m_a g l_a}{p_1 + m_a l_a^2} - \frac{1}{2}\frac{p_2^2}{\left(p_1 + m_a l_a^2\right)^2}}, \tag{79}$$

which, in turn, leads to the following realization of **Step 4**:

Step 4.1: Choose values of arrays $[m_{a_1}, \ldots, m_{a_k}]$, $[l_{a_1}, \ldots, l_{a_n}]$;

Step 4.2: Run numerical experiments and compute

$$\omega_{opt} = \omega_{opt}(m_{a_i}, l_{a_j}), \quad i = 1, \ldots, k, \ j = 1, \ldots, n$$

analyzing the data as proposed following **Steps 1-3**;

Step 4.3: Use statistics (79) for computing estimates for the physical parameters J_p, m_p, l_c, ... of the original set-up or their functions.

If the coefficients are so that the second summand in (79) is much smaller the first one then in **Step 4.3** one can use an alternative approximation

$$\omega_{opt} \approx \sqrt{\frac{p_3 + m_a g l_a}{p_1 + m_a l_a^2}}. \tag{80}$$

Denoting as

$$X_{k,n} = m_{a_k} g l_{a_n}, \quad Z_{k,n} = m_{a_k} l_{a_n}^2, \quad Y_{k,n} = \omega_{opt}^2(m_{a_k}, l_{a_n}), \tag{81}$$

Eqn. (80) can be re-written as a nonlinear regression of the form

$$\boxed{Y_{k,n} = \frac{p_3 + X_{k,n}}{p_1 + Z_{k,n}} + \varepsilon_{k,n}, \qquad k \in K, \ n \in N} \tag{82}$$

and the task can be reformulated as to estimate unknown constants $p_3 >$ and $p_1 > 0$ provided that the values of $Y_{k,n}$, $X_{k,n}$ and $Z_{k,n}$ are available; and then consequently compute both estimates for J_p, m_p, l_c out of the relations

$$p_3 = m_p g l_c, \quad p_1 = J_p + m_p l_c^2 \tag{83}$$

and statistical characteristics of the error ε. Eqn. (82) can be re-written as

$$Y_{k,n} \cdot (p_1 + Z_{k,n}) = p_3 + X_{k,n} + \varepsilon_{k,n} \cdot (p_1 + Z_{k,n}), \qquad k \in K, \ n \in N.$$

and, after re-grouping the terms, it comprises a (almost) linear regression

$$\underbrace{Y_{k,n} \cdot Z_{k,n} - X_{k,n}}_{\text{measured output}} = \overbrace{\begin{bmatrix} \underbrace{\phi_{1_{k,n}}}_{1}, & \underbrace{\phi_{2_{k,n}}}_{(\varepsilon_{k,n} - Y_{k,n})} \end{bmatrix}}^{\text{regressors}} \begin{bmatrix} p_3 \\ p_1 \end{bmatrix} + \overbrace{\underbrace{\delta_{k,n}}_{\varepsilon_{k,n} \cdot Z_{k,n}}}^{\text{new error}} \tag{84}$$

known in literature as *errors-in-variables model*, [2, p. 577]. The specific feature of the model is then a presence of the noise in regressors (independent variables), see the expression of $\phi_{2_{k,n}}$, and dependence of errors present in regressor and additive error in output.

The formulas (79), (82) or (84) assume availability of values for $\omega_{opt}(\cdot)$ computed from analysis of periodograms generated from the data, see **Step 4.2**. However, these (resonance) frequencies should be estimated as well. Indeed, since we might have only a guess of location of a resonance frequency for a given set of parameters of the system, then in running experiments on a physical (or synthetic) system we can enforce and record its response(s) to sinusoidal input(s) with predefined in-advance set of frequencies. Clearly, they should cover an interval where the corresponding resonance frequency is located. However, it is unlikely that we can hit such value by spreading a finite number of frequencies over interval of interest.

There are several alternatives for estimating such frequency from the data. The next algorithm is used in the work

---

Step 4.2.1: Given an interval of frequencies $\left[\Omega_{\min},\, \Omega_{\max}\right]$ that contains yet unknown resonance frequency $\omega_{opt} \in \left[\Omega_{\min},\, \Omega_{\max}\right]$, choose a finite set of frequencies $\omega_k \in \left[\Omega_{\min},\, \Omega_{\max}\right]$, $k = 1, \ldots, K$, which somehow cover the interval and which will be used as parameters for input sine-waves for the nonlinear system (78), e.g. the frequencies ω_k can be equidistantly spread on $\left[\Omega_{\min},\, \Omega_{\max}\right]$;

Step 4.2.2: Record responses of the nonlinear system (78), produce the corresponding estimates for the amplitudes

$$g_k := \left|\widehat{G}(j\omega_k)\right|, \qquad k = 1, \ldots, K$$

and consider their variational series

$$g_{(1)} \leq \cdots \leq g_{(k)} \leq \cdots \leq g_{(K)}; \tag{85}$$

Step 4.2.3: Make up an estimate of ω_{opt} out of the frequencies corresponding to a few top values of variational series. For instance, it can be the frequency of the maximal order statistics $g_{(K)}$

$$\widehat{\omega}_{opt} := \omega\big(g_{(K)}\big);$$

or, it can be a function

$$\widehat{\omega}_{opt} := \mathcal{G}\Big(\big\{g_{(K)}, \omega\big(g_{(K)}\big)\big\}, \ldots, \big\{, g_{(K-1)}, \omega\big(g_{(K-r)}\big)\big\}\Big) \tag{86}$$

of r-frequencies of the r largest elements of the variational series.

The next statement describes the realization of (86) when two largest elements of variational series (85) are used.

Lemma 7 *Given the transfer function*

$$G(s) = \frac{b_0}{s^2 + a_1 \cdot s + a_0}, \qquad b_0 > 0,\ a_1 > 0,\ a_0 > 0 \tag{87}$$

a continuous-in-time second order linear control system (10), suppose its coefficients satisfy the inequality $\left(a_0 - \frac{a_1^2}{2}\right) \geq 0$, *so that the frequency*[6]

$$\omega_{opt} := \sqrt{a_0 - \frac{a_1^2}{2}} \tag{88}$$

represents the argument, where the magnitude of the frequency response function $G\left(j\omega\right)$ *reaches the maximal value*

$$\left|G\left(j\omega_{opt}\right)\right| = \sup_{0 \leq \omega < +\infty} \left|G\left(j\omega\right)\right|.$$

Suppose $\omega_{opt} \in [\Omega_{\min}, \Omega_{\max}]$ *and there are a finite number of frequencies* $\omega_k \in [\Omega_{\min}, \Omega_{\max}]$, $k = 1 \ldots, K$, *for which the values of* $g_k := \left|G\left(j\omega_k\right)\right|$ *are known. Suppose, in addition, that* ω_{opt} *is located in between the frequencies* $\omega\left(g_{(K-1)}\right)$ *and* $\omega\left(g_{(K)}\right)$, *i.e. one of the inequalities*

$$\omega\left(g_{(K-1)}\right) \leq \omega_{opt} \leq \omega\left(g_{(K)}\right), \qquad \omega\left(g_{(K)}\right) \leq \omega_{opt} \leq \omega\left(g_{(K-1)}\right)$$

holds. Then the function

$$\widehat{\omega}_{opt} := \sqrt{\frac{\omega^2\left(g_{(K)}\right) + \omega^2\left(g_{(K-1)}\right)}{2} + \frac{1}{2 \cdot B} \cdot \frac{g_{(K)}^2 - g_{(K-1)}^2}{\omega^2\left(g_{(K)}\right) - \omega^2\left(g_{(K-1)}\right)}} \tag{89}$$

or the function

$$\widehat{\omega}_{opt} := \sqrt{\frac{\omega^2\left(g_{(K)}\right) \cdot \sqrt{g_{(K-1)}^2 + A} + \omega^2\left(g_{(K-1)}\right) \cdot \sqrt{g_{(K)}^2 + A}}{\sqrt{g_{(K-1)}^2 + A} + \sqrt{g_{(K)}^2 + A}}} \tag{90}$$

with

$$A = \frac{b_0}{a_1^2\left[a_0 - \frac{1}{4}a_1^2\right]}, \qquad B = \frac{b_0}{a_1^4\left[a_0 - \frac{1}{4}a_1^2\right]^2} \tag{91}$$

[6] see Lemma 6

provide estimators for the argument of the maximum of $\left|G\left(j\omega_{opt}\right)\right|$ *such that*

$$\left|G\left(j\omega_{opt}\right)\right|^2 - \left|G\left(j\widehat{\omega}_{opt}\right)\right|^2 = o\Big(\left|\widehat{\omega}_{opt} - \omega_{opt}\right|^2\Big).$$

The last means that the Taylor expansion of the left hand side in a vicinity of ω_{opt} *evaluated at* $\widehat{\omega}_{opt}$ *will have trivial terms up to the second order.* ■

Proof: Taking advantage of (74)-(75) and notation $x := \omega^2$, consider the Taylor expansion of $F(\cdot)$ in a vicinity of its maximum at

$$x_{opt} = \omega_{opt}^2 = a_0 - \tfrac{1}{2}a_1^2,$$

defined in Eqns. (75)-(76), i.e.

$$\begin{aligned} F\left(x\right) &= F\left(x_{opt}\right) + \left[\tfrac{d}{dx}F\left(x\right)\right]\Big|_{x=x_{opt}}\left(x - x_{opt}\right) + \\ &\quad + \tfrac{1}{2}\tfrac{d^2}{dx^2}\left[F\left(x\right)\right]\Big|_{x=x_{opt}}\left(x - x_{opt}\right)^2 + o\left(\left|x - x_{opt}\right|^2\right). \end{aligned} \tag{92}$$

Since[7]

$$\begin{aligned} F\left(x\right) &= \frac{b_0}{\left(a_0 - x\right)^2 + a_1^2 x}, \\ \tfrac{d}{dx}F\left(x\right) &= -\frac{b_0\left(2x - 2a_0 + a_1^2\right)}{\left[\left(a_0 - x\right)^2 + a_1^2 x\right]^2} = -\frac{2\cdot b_0\cdot\Big(x - \overbrace{\left[a_0 - \frac{1}{2}a_1^2\right]}^{=x_{opt}}\Big)}{\left[\left(a_0 - x\right)^2 + a_1^2 x\right]^2} \\ &= -\frac{2}{b_0}\cdot F^2\left(x\right)\cdot\left(x - x_{opt}\right). \\ \tfrac{d^2}{dx^2}F\left(x\right) &= -\frac{2}{b_0}\Big[2\cdot F\left(x\right)\cdot\tfrac{d}{dx}F\left(x\right)\cdot\left(x - x_{opt}\right) + F^2\left(x\right)\Big], \end{aligned}$$

then the values of these functions at $x = x_{opt}$ are

$$\begin{aligned} F\left(x_{opt}\right) &= \frac{b_0}{\left(a_0 - \left[a_0 - \frac{1}{2}a_1^2\right]\right)^2 + a_1^2\left[a_0 - \frac{1}{2}a_1^2\right]}, \\ &= \frac{b_0}{a_1^2\left[a_0 - \frac{1}{4}a_1^2\right]} \\ \left[\tfrac{d}{dx}F\left(x\right)\right]\Big|_{x=x_{opt}} &= -\frac{2}{b_0}\cdot F^2\left(x_{opt}\right)\cdot\left(x_{opt} - x_{opt}\right) = 0, \\ \left[\tfrac{d^2}{dx^2}F\left(x\right)\right]\Big|_{x=x_{opt}} &= -\frac{2}{b_0}\cdot F^2\left(x_{opt}\right) = -\frac{2\cdot b_0}{a_1^4\left[a_0 - \frac{1}{4}a_1^2\right]^2} \end{aligned} \tag{93}$$

[7]Here we do not assume that $b_0 = 1$ so that it appears as a factor in all the expressions.

Therefore, the formula (92) becomes equivalently re-written as

$$F(x) = \overbrace{\frac{b_0}{a_1^2\left[a_0 - \frac{1}{4}a_1^2\right]}}^{=:\,A} - \overbrace{\frac{b_0}{a_1^4\left[a_0 - \frac{1}{4}a_1^2\right]^2}}^{=:\,B} \cdot \left(x - \left[a_0 - \tfrac{1}{2}a_1^2\right]\right)^2 + o\left(\left|x - \left[a_0 - \tfrac{1}{2}a_1^2\right]\right|^2\right). \tag{94}$$

If the set of testing frequencies ω_k is chosen sufficiently dense on $[\Omega_{\min}, \Omega_{\max}]$, then the values of $F(\cdot)$ at $x_{(K)} = \omega^2\left(g_{(K)}\right)$ and $x_{(K-1)} = \omega^2\left(g_{(K-1)}\right)$ are close to $g_{(K)}^2$ and $g_{(K-1)}^2$ respectively. Hence the Taylor expansion (94) leads to the following relations

$$F\left(x_{(K)}\right) \approx g_{(K)}^2 \approx A - B \cdot \left(x_{(K)} - x_{opt}\right)^2 \tag{95}$$

$$F\left(x_{(K-1)}\right) \approx g_{(K-1)}^2 \approx A - B \cdot \left(x_{(K-1)} - x_{opt}\right)^2 \tag{96}$$

where A and B are introduced for brevity of expressions in (94). If we consider the approximations (95) and (96) as equalities, then we obtain the next identity

$$g_{(K)}^2 + B \cdot \left(x_{(K)} - x_{opt}\right)^2 = g_{(K-1)}^2 + B \cdot \left(x_{(K-1)} - x_{opt}\right)^2,$$

which, in turn, implies

$$\begin{aligned} g_{(K)}^2 - g_{(K-1)}^2 &= B \cdot \left(x_{(K-1)} - x_{opt}\right)^2 - B \cdot \left(x_{(K)} - x_{opt}\right)^2 \\ &= B \cdot \Big[\left(x_{(K-1)} - x_{opt}\right) - \left(x_{(K)} - x_{opt}\right)\Big] \\ &\qquad \times \Big[\left(x_{(K-1)} - x_{opt}\right) + \left(x_{(K)} - x_{opt}\right)\Big] \\ &= B \cdot \Big[x_{(K-1)} - x_{(K)}\Big] \cdot \Big[x_{(K-1)} + x_{(K)} - 2 \cdot x_{opt}\Big]. \end{aligned}$$

The last formula suggests the next approximation for unknown value

$$x_{opt} \approx \frac{x_{(K)} + x_{(K-1)}}{2} + \frac{1}{2 \cdot B} \cdot \frac{g_{(K)}^2 - g_{(K-1)}^2}{x_{(K)} - x_{(K-1)}}, \tag{97}$$

which is (asymptotically) unbiased for the argument of the maximum of the amplitude of the frequency response function $\left|G\left(j\omega_{opt}\right)\right|$.

Alternatively, two equations resulted from the relations (95) and (96) lead also to the other identity

$$\frac{g_{(K-1)}^2 + A}{g_{(K)}^2 + A} = \frac{\left(x_{(K-1)} - x_{opt}\right)^2}{\left(x_{(K)} - x_{opt}\right)^2}.$$

It can be re-written as the second order equation w.r.t. x_{opt}. Namely,

$$\begin{aligned} 0 &= \left[g^2_{(K-1)} + A\right] \cdot \left(x_{(K)} - x_{opt}\right)^2 - \left[g^2_{(K)} + A\right] \cdot \left(x_{(K-1)} - x_{opt}\right)^2 \\ &= \left[\sqrt{g^2_{(K-1)} + A} \cdot \left(x_{(K)} - x_{opt}\right) - \sqrt{g^2_{(K)} + A} \cdot \left(x_{(K-1)} - x_{opt}\right)\right] \\ &\quad \times \left[\sqrt{g^2_{(K-1)} + A} \cdot \left(x_{(K)} - x_{opt}\right) + \sqrt{g^2_{(K)} + A} \cdot \left(x_{(K-1)} - x_{opt}\right)\right] \end{aligned}$$

It has two solutions and the only one is relevant to the estimate of x_{opt}. It is

$$x_{opt} \approx \frac{\alpha \cdot x_{(K)} + \beta \cdot x_{(K-1)}}{\alpha + \beta}, \qquad \alpha = \sqrt{g^2_{(K-1)} + A},\ \beta = \sqrt{g^2_{(K)} + A}, \quad (98)$$

where A is defined in (94). Both formulas (97) and (98) re-written in the original variables are given in the statement as (89) and (90) respectively. ■

Apparent limitation of the formulas (89) and (90) is that they are explicitly dependent on parameters of the model in the form of the lumped coefficients A and B given in Eqn. (91). The next modification of one of these formulas helps to remove the obstacle

Theorem 2 *Consider a continuous-in-time second order linear control system (10) with the transfer function*

$$G(s) = \frac{b_0}{s^2 + a_1 \cdot s + a_0}, \qquad b_0 > 0,\ a_1 > 0,\ a_0 > 0, \quad (99)$$

and suppose all the settings of Lemma 7 are valid. Then the function

$$\widetilde{\omega}_{opt} := \sqrt{\frac{\omega^2\big(g_{(K)}\big) \cdot \sqrt{\frac{g^2_{(K-1)}}{g^2_{(K)}} + 1} + \omega^2\big(g_{(K-1)}\big) \cdot \sqrt{2}}{\sqrt{\frac{g^2_{(K-1)}}{g^2_{(K)}} + 1} + \sqrt{2}}} \quad (100)$$

provide estimators for the argument of the maximum of $\left|G\big(j\omega_{opt}\big)\right|$ such that

$$\left|G\big(j\omega_{opt}\big)\right|^2 - \left|G\big(j\widetilde{\omega}_{opt}\big)\right|^2 = o\Big(\left|\widetilde{\omega}_{opt} - \omega_{opt}\right|^2\Big).$$

The last means that the Taylor expansion of the left hand side in a vicinity of ω_{opt} evaluated at $\widetilde{\omega}_{opt}$ will have trivial terms up to the second order. ■

Proof immediately comes from Lemma 7 and the observation that in notations of proof of Lemma 7 the constant A and the value of the function $F(\cdot)$ at x_{opt} – appeared in Eqns. (91) and (93) – coincide, $A = F(x_{opt})$. Indeed, the square of the maximal order statistics $g_{(K)}$ of the variational series (85) approaches $F(x_{opt})$, when we consider an increasing (in number of elements) sets of testing frequencies ω_k that are well-spread and cover the interval $\left[\Omega_{\min}, \Omega_{\max}\right]$. Therefore, if one divides the numerator and denominator of the function (90) by $g_{(K)}$, then s/he obtains its equivalent form

$$\widehat{\omega}_{opt} = \sqrt{\frac{\omega^2\big(g_{(K)}\big) \cdot \sqrt{\frac{g^2_{(K-1)}}{g^2_{(K)}} + \frac{A}{g^2_{(K)}}} + \omega^2\big(g_{(K-1)}\big) \cdot \sqrt{1 + \frac{A}{g^2_{(K)}}}}{\sqrt{\frac{g^2_{(K-1)}}{g^2_{(K)}} + \frac{A}{g^2_{(K)}}} + \sqrt{1 + \frac{A}{g^2_{(K)}}}}} \tag{101}$$

However, taking into account the mentioned above arguments on converging $g^2_{(K)}$ to $F(x_{opt}) = A$ for increasing a number of well-spread testing frequencies, we can conclude that in limit the expression (101) approaches (100). ■

New statistics $\widetilde{\omega}_{opt}$ for estimating resonance frequency ω_{opt} have been tested on synthetic data to validate its use in analysis of the experiments and its relevance in drawing conclusions. Results of some numerical tests and comments are presented in Table 1 and its caption.

Mass m_a	**Length** l_a	ω_{opt} **from Eqn.** (79)	$\widetilde{\omega}_{opt}$ **from Eqn.** (100)
0	0	3.8788	3.7740
0.05	0.005	4.0671	3.7705
0.1	0.01	4.4156	4.0492
0.15	0.015	4.8812	4.4680
0.2	0.02	5.4194	5.0265

Table 1: Numerical results for estimating optimal frequency ω: The results above highlight the estimates obtained following **Step 4** for determining the optimal value of ω_{opt}. The first two columns show the varying values of the additional mass and length, denoted as m_a and l_a, respectively. The third column presents the optimal frequency ω_{opt} calculated using the full model as per Eqn. (79), which assumes full knowledge of the parameters p_1 - p_4. In contrast, the fourth column provides the estimate $\widetilde{\omega}_{opt}$ obtained from Eqn. (100), where the parameters p_1 - p_4 are unknown. While the estimates $\widetilde{\omega}_{opt}$ deviate from the true optimal values, the approximation's accuracy is evident.

With new data-driven estimate $\widetilde{\omega}_{opt}$ of ω_{opt} proposed by Eqn. (100), we

can turn to **Step 4.3** and discuss numerical procedures for computing estimates for some of parameters p_1-p_4 of the nonlinear system (5). The first alternative here is to consider the reduced model (82) and the corresponding non-standard linear regression (84) for parameters fitting. As the second alternative, one can consider the full model (79) and search the parameters by solving the constrained optimization assignment minimizing the value of the data-driven loss function $f = f(p_1, p_2, p_3)$, which is naturally defined as the sum of squared mismatches of the resonant frequencies of the linearized dynamics and their data-driven estimates $\widetilde{\omega}_{opt}(\cdot)$ given by Eqn. (100)

$$f(\cdot) := \sum_{k,n} \left| \widetilde{\omega}^2_{opt}(m_{a_k}, l_{a_n}) - \left\{ \frac{p_3 + m_{a_k} g l_{a_n}}{p_1 + m_{a_k} l^2_{a_n}} - \frac{1}{2} \frac{p_2^2}{\left(p_1 + m_{a_k} l^2_{a_n}\right)^2} \right\} \right|^2 \tag{102}$$

The constraints – under which the function $f(\cdot)$ is to be minimized – are reflecting prior guesses on intervals of physical parameters of the system converted to the bounds imposed on unknown constants p_1-p_3.

Remark 6 In the synthetic case, one may consider the known parameter values presented previously in Eqn. (62) along with the values presented in Table 1, in order to minimize Eqn. (102) and subsequently estimate p_1, p_2, p_3. Further, given the physical nature of the parameters we know approximately which upper and lower bounds to use when iterative searching for the optimal estimates. ■

Parameters	p_1	p_2	p_3	low/upp bound
Estimated values (only p_1 and p_3)	0.0033	–	0.0453	(0,0);
Real values (only p_1 and p_3)	0.0033	–	0.0491	(1,1)
Estimated values (p_1, p_2, and p_3)	0.0033	0.0100	0.0606	(0,0,0);
Real values (p_1, p_2, and p_3)	0.0033	0.0010	0.0491	(p_1, p_2, p_3)*10

Table 2: Comparison of Estimated and Real Parameter Values for p_1, p_2, and p_3 using Eqn (102) with constraints bounding the estimates from below and above.

Solving the optimization problem presented in Eqn. (102) was done using the fmincon function in MATLAB and the results of the estimates are presented within Table 2. Firstly, a simpler task of only solving for p_1, p_3 was performed for a given constant p_2. Secondly, optimizing for an estimate p_1 - p_3 was executed. Glancing at the aforementioned Table, one can indeed see the estimates greatly approximating the synthetic real values, especially of

p_1 - yielding an excellent point estimate in both estimation procedures. p_3 is underestimated initially by roughly 10%, followed by an overestimation by 25% of the real value. Even though, there are room for improvement - as an initial stage estimation that could be built upon in a iterative manner, the p_3 estimate falls within reasonable range from its true value. Lastly, adding additional complexity by proceeding with estimating p_2, one immediately sees that p_2 has a 10 fold numerical deviation from its real synthetic value and it simultaneously worsen the estimate for p_3. In addition, the upper bound limit was reached for p_2 and would most likely have deviated further if it weren't for the constraints. Therefore treating the estimate of p_2 as unreliable, given our laid out intuition and knowledge of the real values is a reasonable assumption.

Naturally, when dealing with few data points and small sample sizes, in our case 5 different masses and lengths as shown in Table 1, increasing the number of variability of m_a, l_a in a synthetic simulation environment can be executed rapidly, and will most definitely produce highly accurate results. Omitting and preventing the issues seen with estimating p_2. However, recording samples in a real life robotic set ups more often than not are limited by financial, time and physical constraints. Subsequently, evaluating the performance of estimates on a smaller realistically replicated sample size is in line with practical real world applications.

Yet, this is still a great achievement and result - in-spite of poor performance of p_2, reliably predicting some of the lumped variables within a reasonable range of deviation and extracting useful knowledge of the system based solely of the measurements outlined in Eqn. (102) can be exploited to perform inference and parameter identification on real-world robotic systems, which is covered and applied in Section (3).

3 The case study: identification of parameters of the dynamics of the Butterfly robot

All **Steps 1-4** of Section 2 have been applied for identification of parameters of the 1st degree of freedom of the Butterfly robot outlined concisely in Section (1) with minor modifications. They are commented next.

3.1 Step 1: Choose the ranges of amplitudes and frequencies of input and record responses

Considering the nonlinear dynamics of the Butterfly robot and the need for precise calibration, the choice of input signal amplitudes and frequencies should be selected in a delicate manner in order to ensure that the system's response remains within the linear range near the stable equilibrium of the nonlinear system, in line with arguments presented in Section (2.3.1). As before, the amplitudes of the input sin-waves have been chosen small enough to keep forced oscillations of the system in the range of small oscillation, e.g. avoiding performing too large and hastily forced motion which would present an increased complexity in identifying the parameters.

Unlike the synthetic case, the added mass $m_a = \left[0.052, 0.1205, 0.154\right]$ (kg), are limited to three variations and furthermore no changes to l_a could be made due to physical constraints - limiting the length to 104 (mm).

Frequency (rad/sec)	**Amp: 52 g**	**Amp: 120.5 g**	**Amp: 154 g**
2.0	0.008	-	-
2.5	0.008	-	-
3.0	0.006	0.015	-
3.5	0.005	0.010	0.015
4.0	0.003	0.010	0.015
4.5	0.003	0.010	0.015
4.75	-	0.010	-
5.0	0.003	0.010	0.008
5.5	0.004	0.008	0.004
6.0	0.010	0.004	0.003
6.5	-	0.006	0.006
7.0	-	0.010	0.010
7.5	-	-	0.020
8.0	0.020	-	-
10.0	0.040	0.020	0.060
12.0	0.060	0.040	0.080
14.0	0.080	0.070	0.100
16.0	0.100	0.100	-

Table 3: Frequency and Amplitude values selected for 52 grams, 120.5 grams, and 154 grams of m_a, aimed at encompassing the frequencies around the natural frequency of the system. Therefore, slight modifications are done to amplitude as well as selection of frequencies for each value.

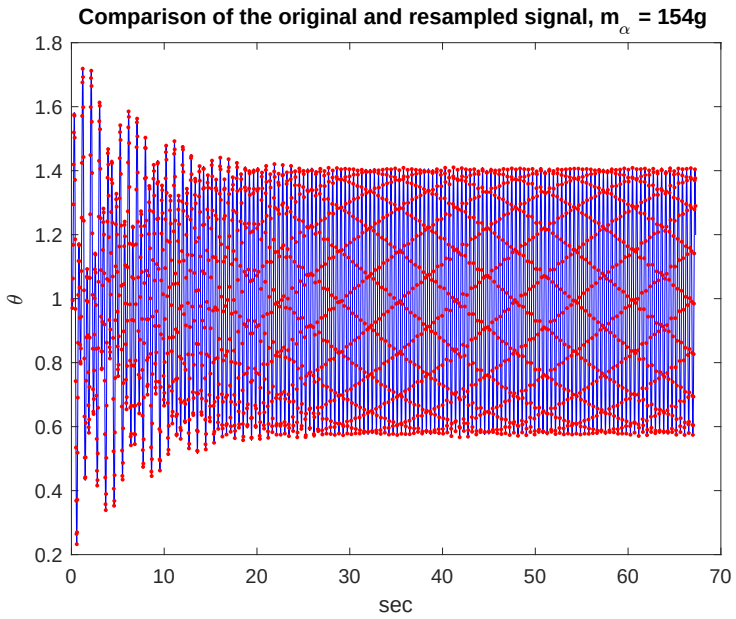

Figure 9: (Non-centered) response of nonlinear system to sin-input $v(t) = A \cdot \sin(\omega \cdot t)$ with $\omega = 14[rad/sec]$, $A = 0.1$ is depicted in blue; red dots illustrate the resampling of the response at an 0.04 *sec* rate, which used further in analysis.

Data collection process is done by attachment of added masses, followed by sending sin-inputs of $v(t) = A \cdot \sin(\omega \cdot t)$ with ω, A as taken from Table 3. Subsequently, recording the the forced oscillations as seen in Fig. (9) for input various inputs. As it provides a graphical representation into how the system reacts. Similar figures can be illustrated by all m_a specified but omitted from the text due to redundancy. Key point remains that the first 30 seconds are discarded as a transition period to the steady-state oscillations, whilst the remainder is used for the identification of parameters.

3.2 Step 2: Process the data and obtain the periodograms of signals

Processing redundant and noisy collected data is essential for reducing the complexity and increasing the accuracy of the parameter identification process. Judging by Fig. 10, one can instantly observe the issue of noisy data. In fact, it may be inferred that our data could be unreliable due to the uncertainty in the time stamps at which the data points were recorded. To mitigate this, the dataset is resampled at a rate of 0.04 *sec*, ensuring evenly spaced data points, as illustrated by the red dots in Fig. 9. This is followed

by truncating the data to focus solely on the stable system behavior, which is crucial for the accurate modeling of the system dynamics.

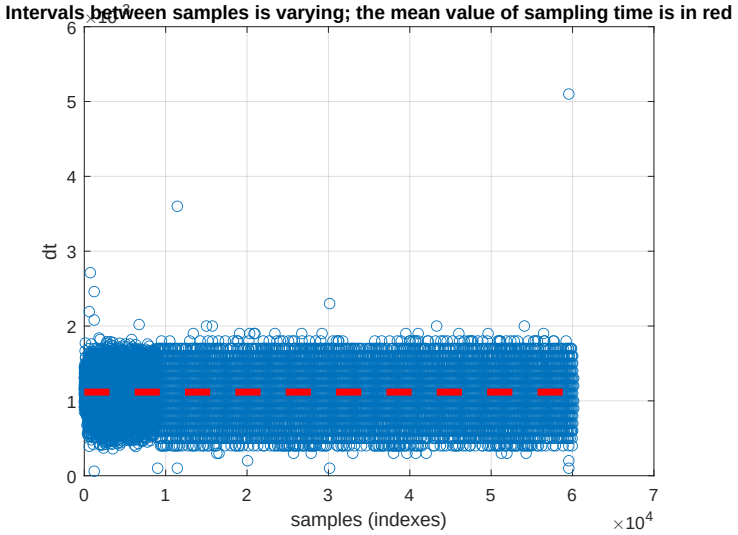

Figure 10: The figure illustrates the irregularity within the samples recorded for $m_a = 0.154$ (kg), implying unreliability and/or uncertainty of the quality of the data collected. Notice the concentration of dots slightly above 0.001 $[sec]$, whilst the 'stripe like' pattern from 1 and onward.

The next step involves computing the periodogram for the DFT of the resampled, nearly steady-state responses. The periodogram reveals a strong non-zero peak close to a dominant frequency, as shown in Fig. 11. This peak then provides insight into the system's frequency response.

From the frequency response, we estimate the system's transfer function $G_p(z)$ by the steps shown in Section 2.3.3. The transfer function characterizes the relationship between the input and output of the system in the frequency domain and plays a great role in identifying the system's dynamic behavior. For the nonlinear system under study, each resampled response requires the computation of the transfer function to capture the system's behavior in the vicinity of a particular point.

3.3 Step 3: Compute estimate for $G_p(z)$

Following the steps covered in the synthetic case, we proceed with estimating the transfer function $G_p(z)$ based on Eqn. (68). Further, proceeding with plotting the estimated values for amplitude - which approximates the underlying transfer function. Fig (3.3) shows the estimated transfer function values of $G_p(z)$ plotted for every m_a.

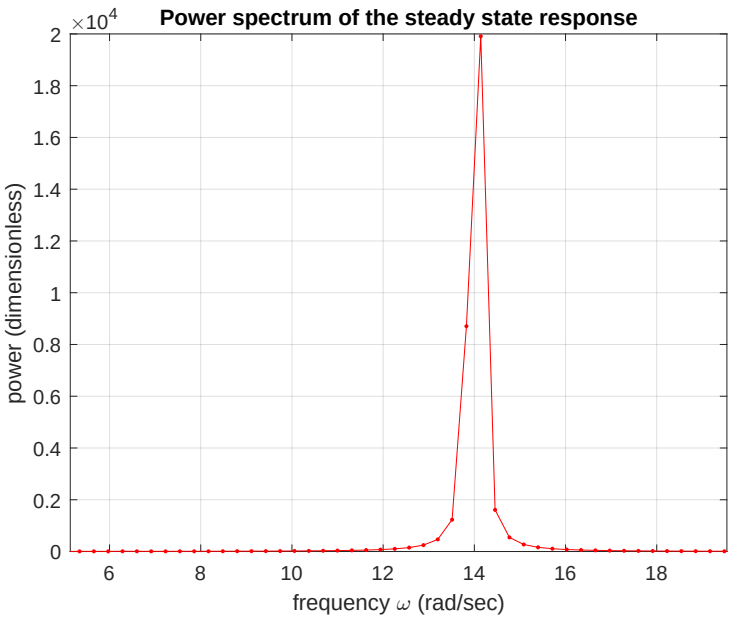

Figure 11: The periodogram for a resampled response ($m_\alpha = 154$g) of a nonlinear system. A dominant frequency can be observed at $\omega = 14$ *(rad/sec)* together with non-negligible peak slightly below that frequency.

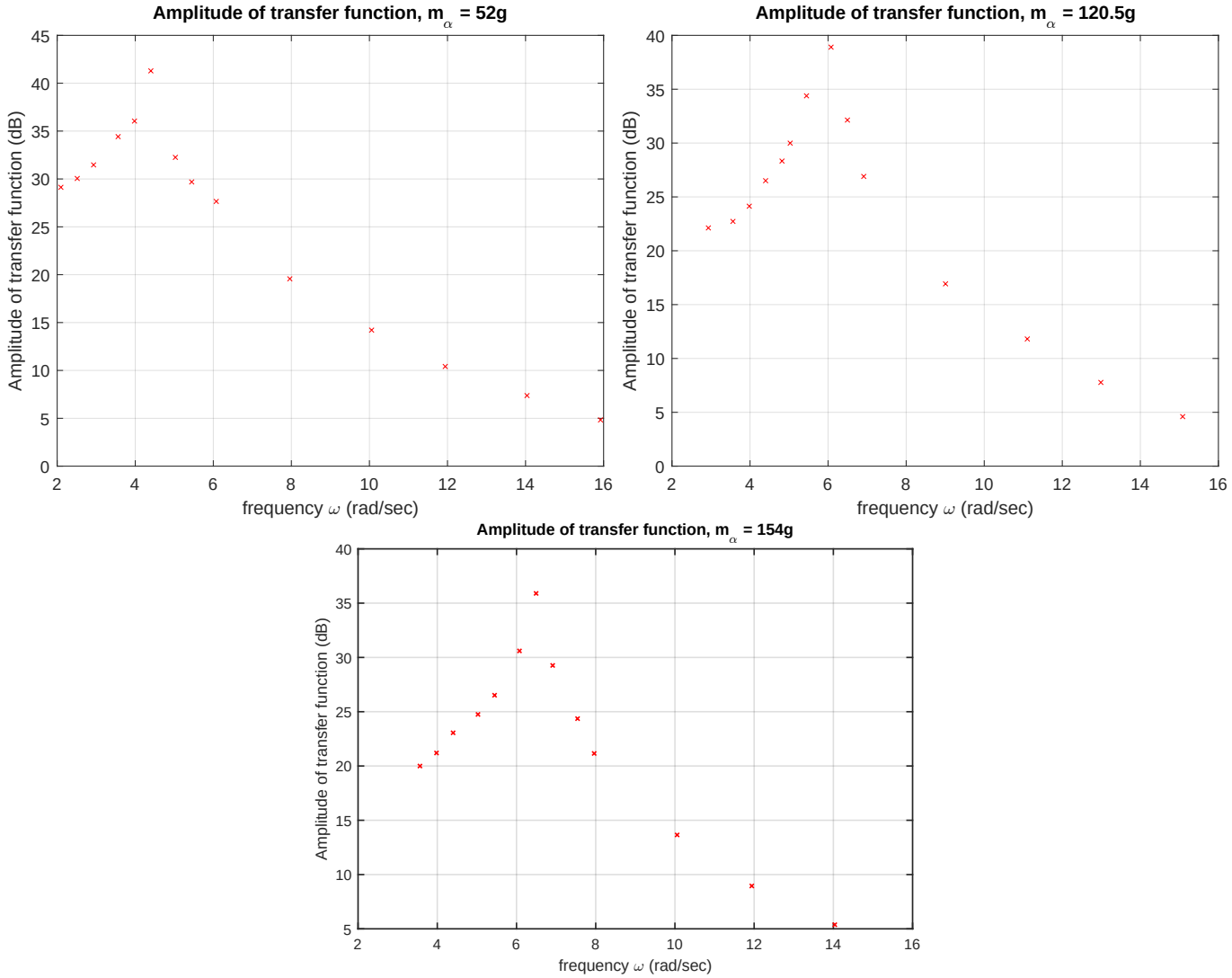

Figure 12: The figure covers three plots with estimated values of magnitudes of the underlying transfer functions for each of the different values of added mass $m_a = \left[0.052,\, 0.1205,\, 0.154\right]$ (kg), reconstructed based on Eqn. (68.

3.4 Step 4: Deriving estimates for the parameters p_1-p_4 or their functions

Having collected the data in Step 1, processed it in Step 2, estimated a transfer function with different frequency values as well as amplitude values in Step 3. Then, one continues with deriving the optimal values and parameter estimates utilizing by Eqn. (100). Estimating the optimal omega $\widetilde{\omega}_{opt}$ using previously acquired in Step 3 values for frequency $\omega(g(k))$ and amplitude g(k).

Computing the values of $\widetilde{\omega}_{opt}$ for each m_a yields the following results

Mass (grams)	**Optimal Omega: $\widetilde{\omega}_{opt}$ (rad/sec)**
52.0	4.1915
120.5	5.7650
154.0	6.2847

Table 4: Optimal Omega estimates for different weights in m_α

Lastly, using the values from Table 4 and applying them to Eqn. (102), one can utilize the constraint optimization function fmincon within MATLAB to minimize the objective function given some constraints.

Parameters	p_1	p_2	p_3	low/upp bound
Estimated values	0.0028	0.0188	0.0583	(0,0,0); (0.1,0.02,4)

Table 5: Estimated Parameter Values for p_1, p_2, and p_3 using Eqn (102) with constraints bounding the estimates from below and above.

Loosely speaking, for practical purposes it is not possible to know the true value as we did in the synthetic case using Eqn. (79), however from practice one may get a sense of order of magnitude. Based on previous (alternative) case studies both estimates for parameters p_1 and p_3 is expected to be within the same vicinity as the real yet-unknown values. However, just as in the synthetic case - in the real world application the estimate for p_2 is believed to be off by a order of $10-20$ fold, in other words, there is room for improvement.

4 Methods for re-calibrating the robot dynamics in a vicinity of its motion

As commented and discussed above, the task of calibrating parameters of the dynamics even of the simplest robotic system can be a non-trivial assignment. Furthermore, since a model of the dynamics of the physical robot is expected to be *generic*, i.e. valid for describing arbitrary forced motion, then the use of such an approximate (grey-box) model in planning and performing *particular motions* – when realized on the physical robot – might lead to *modest* performance.

In supporting the last point, one can trace and compare characteristics on *path accuracy* and *position accuracy* of industrial robot manipulators available on the market. Both are rarely simultaneously mentioned, but if quoted, then *path accuracy* is often of 10-fold or more of the robot *position accuracy*. The reason for that inconsistency of motion dependent versus static robots' performance is readily linked to quality of *generic* models of the robot dynamics. Indeed, for improving position accuracy of a robot the detailed model of dynamics is not necessary and the knowledge of its first order approximation at a given regulated point is sufficient. Meanwhile, for improving path following and consequently reference tracking ability of the robot, an accurate model of its dynamics is required. If such model is just a *generic* approximation of the physical robotic system and possesses structural and non-structural uncertainties, then it is unlikely that such effects can be completely mitigated by an appropriate controller design.

As a reasonable step forward in improving *path accuracy* and path following of a robotic system, one can search for *motion dependent* parametric models that are covering the dynamics of the system in tubular neighbourhoods of individual forced motions.

The main contribution of the thesis provides novel arguments and an example in deriving such model and, specifically, in deriving new formats of *linear regression* for those parameters of the systems that are primarily responsible for characterizing the system dynamics in a tubular vicinity of a pre-defined forced motion. The background idea for developing new classes of motion-dependent models comes from the observation that

- each individual forced motion of a nonlinear system possesses a rich set of motion-dependent invariants; and
- analysis of first-order approximation of these quantities can be used for calibration of the system dynamics, if such step is appropriate.

4.1 Re-calibration of the dynamics of the 1st degree of freedom of the Butterfly robot in a vicinity of its oscillation

As the case study, let us consider a trajectory $\theta_*(t)$ defined as a periodic oscillation of the nonlinear system (5) of constant energy (if friction would be absent) of maximal inclination $\theta_{\max}$ from the vertical and consider *the problem of orbital stabilization of this specific motion.* If true parameters p_1-p_3 and the controller gain p_4 of the system would be available, $\tau_\varepsilon(\cdot) \equiv 0$ and the model for the dynamics of the pendulum is indeed correct, then we can directly compensate for the viscous friction by adding the corresponding feed-forward term to the control variable

$$v(t) = v_{new}(t) + \frac{p_2}{p_4} \cdot \dot{\theta}(t) \tag{103}$$

and bring the system's dynamics (5) to the form

$$p_1 \cdot \ddot{\theta}(t) + p_3 \cdot \sin\big(\theta(t)\big) = p_4 \cdot v_{new}(t). \tag{104}$$

The mechanical energy $E(\cdot)$ of (104) if $v_{new}(\cdot)$ would be zero has the form

$$E\big(\theta, \dot{\theta}\big) := \frac{p_1}{2} \cdot \dot{\theta}^2 + p_3 \cdot \big(1 - \cos(\theta)\big). \tag{105}$$

It can be readily seen that for any solution $\theta(t) = \theta\big(t, \theta_0, \dot{\theta}_0\big)$ of (104) with zero control input $v_{new}(\cdot)$ the time function

$$E(t) := E\big(\theta, \dot{\theta}\big)\Big|_{\theta=\theta(t),\, \dot{\theta}=\dot{\theta}(t)} \tag{106}$$

does not change its value. Indeed, computing the time derivative of $E(t)$ and taking advantages of the chain rule and the dynamics (104) results in

$$\begin{aligned}
\frac{d}{dt}E(t) &= \frac{p_1}{2} \cdot 2 \cdot \dot{\theta}(t) \cdot \ddot{\theta}(t) + p_3 \cdot \sin\big(\theta(t)\big) \cdot \dot{\theta}(t) \\
&= \dot{\theta}(t) \cdot \underbrace{\Big[p_1 \cdot \ddot{\theta}(t) + p_3 \cdot \sin\big(\theta(t)\big)\Big]}_{\text{Right-hand side of (104)}} = \dot{\theta}(t) \cdot \Big[p_4 \cdot \underbrace{v_{new}(t)}_{\text{Assumed } \equiv 0}\Big] \\
&= 0
\end{aligned}$$

and, therefore, $E(t) \equiv E(0)$ even though the solution $\theta(t)$ – used in computing $E(t)$ – is varying over the time. In this way, the function

$$I\big(\theta, \dot{\theta}, \theta_{0*}, \dot{\theta}_{0*}\big) := E\big(\theta, \dot{\theta}\big) - E\big(\theta_{0*}, \dot{\theta}_{0*}\big) \tag{107}$$

becomes a motion dependent quantity (often called in literature as an invariant of the motion) that is zero on the nominal motion $\theta_*(t)$ of the unforced system (104) with initial conditions at $[\theta_{0*}, \dot{\theta}_{0*}]$ and which is non-zero for all points of state of the system outside of the orbit of the nominal motion.

As originally reported in [3, 12], the feedback controller designed based on use of the function (107) can render the nominal motion of the unforced system (104) asymptotically orbitally stable.

Lemma 8 *Given a point* $[\theta_{0*}, \dot{\theta}_{0*}]$ *with*[8]

$$E\big(\theta_{0*}, \dot{\theta}_{0*}\big) \neq 0 \quad or \quad E\big(\theta_{0*}, \dot{\theta}_{0*}\big) \neq 2 \cdot p_3, \tag{108}$$

where $E(\cdot)$ *is defined by Eqn. (105), consider the closed loop system consisting of the nonlinear system (104) and of the feedback controller*

$$v_{new} = -\gamma \cdot \dot{\theta}(t) \cdot \Big[E\big(\theta(t), \dot{\theta}(t)\big) - E\big(\theta_{0*}, \dot{\theta}_{0*}\big)\Big] \tag{109}$$

with γ *being a positive constant,* $\gamma > 0$*, then the solution* $\theta(t) = \theta\big(t, \theta_{0*}, \dot{\theta}_{0*}\big)$ *of such closed-loop system (104), (109) originated at the point* $[\theta_{0*}, \dot{\theta}_{0*}]$ *is asymptotically orbitally stable.* ■

Proof can be found in the mentioned above references and based on analysis of time evolution of the following non-negative function

$$V(\theta, \dot{\theta}) := \Big[E\big(\theta, \dot{\theta}\big) - E\big(\theta_{0*}, \dot{\theta}_{0*}\big)\Big]^2$$

along a solution of the closed-loop system (104), (109). ■

Clearly, any solution of the unforced nonlinear system (104) with initial conditions that meet the property (108), is a periodic oscillation. At a first glance, a presence of (orbitally) stable periodic oscillations in the dynamics of the nonlinear system (104), (109) is similar to the presence of a forced periodic oscillation in response to a sin-wave input explored in Sections 2 and 3. However, the periodic motion mentioned in Lemma 8 differs from induced oscillations in many aspects. For instance,

- such stable oscillation of the closed-loop system can be of large amplitude and its presence cannot be detected by linearization of the closed loop dynamics about the equilibrium at $\theta_e = 0$ as done in Lemma 1;

[8] The condition excludes the initial conditions that correspond to the downward and upright equilibriums of the friction-free physical pendulum, which dynamics are given in the left-hand side of (104).

- such stable oscillation of the closed-loop system (104), (109) represents the truly non-linear phenomenon and cannot be approximated by a sine-wave of scaled amplitude as done in Lemma 2; and *etc.*

The next statement forms the basis for calibrating the dynamics of the closed loop system in a vicinity of the nominal oscillation.

Theorem 3 *Consider the nominal T-periodic solution $\theta_*(t) = \theta_*\big(t, \theta_{0*}, \dot\theta_{0*}\big)$, $\theta_*(t) = \theta_*(t+T)$, $\forall\, t$, of the closed-loop system (104), (109) run under conditions of Lemma 8, and consider a perturbed solution*

$$\theta_p(t) = \theta_p\big(t, \theta_{0*} + \varepsilon_1, \dot\theta_{0*} + \varepsilon_2\big)$$

of the closed-loop system, then the value of the function $I(\cdot)$ defined by (107) and evaluated on a solution $\theta_p(t)$, i.e.

$$I\big(\theta_p(t), \dot\theta_p(t), \theta_{0*}, \dot\theta_{0*}\big) = E\big(\theta_p(t), \dot\theta_p(t)\big) - E\big(\theta_{0*}, \dot\theta_{0*}\big) \tag{110}$$

can be approximated by a solution $y(\cdot)$ of the linear differential equation

$$\tfrac{d}{dt} y(t) = a(t) y(t) \tag{111}$$

with the scalar T-periodic coefficient $a(\cdot)$ defined as

$$a(t) := -p_4 \cdot \gamma \cdot \big[\dot\theta_*(t)\big]^2 \tag{112}$$

in the following sense:

$$\lim_{t \to +\infty} \frac{I\big(\theta_p(t), \dot\theta_p(t), \theta_{0*}, \dot\theta_{0*}\big)}{y(t)} = 1, \tag{113}$$

provided that the constants ε_1 and ε_2, which define the shift of initial conditions of the perturbed solution from the nominal one, are chosen small enough. ■

Proof: In order to validate the statement, consider a perturbed solution $\theta_p(\cdot)$ of the closed system (104), (109) and compute the time derivative of the

function $I(\cdot)$ defined by Eqn. (110) along this solution. Namely,

$$\begin{aligned}
\frac{d}{dt}I\big(\theta_p(t),\dot\theta_p(t),\theta_{0*},\dot\theta_{0*}\big) \;&=\; \frac{d}{dt}E\big(\theta_p(t),\dot\theta_p(t)\big)-\underbrace{\frac{d}{dt}E\big(\theta_{0*},\dot\theta_{0*}\big)}_{=\,0}\\
&=\; \underbrace{\Big[\frac{\partial}{\partial\theta}E\big(\theta,\dot\theta\big)\Big|_{\theta=\theta_p(t),\dot\theta=\dot\theta_p(t)}\Big]}_{=\,p_3\cdot\sin\left(\theta_p(t)\right)}\cdot\frac{d\theta_p}{dt}+\underbrace{\Big[\frac{\partial}{\partial\dot\theta}E\big(\theta,\dot\theta\big)\Big|_{\theta=\theta_p(t),\dot\theta=\dot\theta_p(t)}\Big]}_{=\,p_1\cdot\dot\theta_p(t)}\cdot\frac{d\dot\theta_p}{dt}\\
&=\; \dot\theta_p(t)\cdot\Big[p_1\cdot\ddot\theta_p(t)+p_3\cdot\sin\big(\theta_p(t)\big)\Big] \;=\; \dot\theta_p(t)\cdot\Big[\;\underbrace{p_4\cdot v_{new}(t)}_{\text{see Eqn. (104)}}\;\Big]\\
&=\; \dot\theta_p(t)\cdot\Big[\underbrace{-\,p_4\cdot\gamma\cdot\dot\theta_p(t)\cdot\Big[E\big(\theta_p(t),\dot\theta_p(t)\big)-E\big(\theta_{0*},\dot\theta_{0*}\big)\Big]}_{\text{see Eqn. (109)}}\Big]\\
&=\; -\,p_4\cdot\gamma\cdot\dot\theta_p^2(t)\cdot I\big(\theta_p(t),\dot\theta_p(t),\theta_{0*},\dot\theta_{0*}\big)
\end{aligned}$$

This differential relation can be formally in the format

$$\frac{dI(t)}{I(t)}=-\,p_4\cdot\gamma\cdot\dot\theta_p^2(t)$$

and integrated over time interval $[0,\tau]$ resulting in

$$I\big(\tau\big)=\exp\Big[-\,p_4\cdot\gamma\cdot\int_0^\tau\dot\theta_p^2(t)dt\Big]\cdot I\big(0\big),\tag{114}$$

where in the last two equations for brevity we have used the notation

$$I(s):=I\big(\theta_p(s),\dot\theta_p(s),\theta_{0*},\dot\theta_{0*}\big).$$

Asymptotic orbital stability of the nominal T-periodic solution $\theta_*(t)$ of the closed loop system (104), (109) stated in Lemma 8, implies the convergence of the perturbed solution $\theta_p(t)$ to the nominal one in the following sense: for any perturbed solution of the closed loop system there is a constant ψ_0 commonly referred to as an asymptotic phase shift, which is different for different perturbed solutions, so that

$$\lim_{t\to\infty}\big|\theta_p(t)-\theta_*(t+\psi)\big|=0.$$

Clearly, the last relation implies the similar "limit property" for the derivatives, and, hence,

$$\lim_{\tau\to\infty} \frac{\int\limits_0^\tau \dot\theta_p^2(t)dt}{\int\limits_0^\tau \dot\theta_*^2(t)dt} = 1.$$

This immediately implies the validity of the statement. Indeed, any solution $y(t)$ of the linear differential equation (111) has the form

$$y(t) = \exp\Big[-p_4\cdot\gamma\cdot\int\limits_0^\tau \dot\theta_*^2(t)dt\Big]\cdot y(0).$$

Therefore,

$$\lim_{t\to+\infty}\frac{I\big(\theta_p(t),\dot\theta_p(t),\theta_{0*},\dot\theta_{0*}\big)}{y(t)} = \lim_{t\to+\infty}\frac{\exp\Big[-p_4\gamma\int\limits_0^t\dot\theta_p^2(t)dt\Big]\cdot I\big(0\big)}{\exp\Big[-p_4\gamma\int\limits_0^t\dot\theta_*^2(t)dt\Big]\cdot y\big(0\big)} = \frac{I\big(0\big)}{y\big(0\big)}$$

To complete the proof, one can choose the initial condition to the linear system (111) to make the last fraction equals to one. ∎

The direct consequence of Theorem 3 is an ability to substitute the continuous-in-time comparison linear system by discrete-in-time linear approximation as done next.

Lemma 9 *Suppose the settings of Theorem 3 are hold. Consider a perturbed solution $\theta_p(t)$ of the closed-loop system (104), (109)) with the initial conditions at $\theta_p(0)$, $\dot\theta_p(0)$ and chosen close enough to the orbit of the nominal motion $\theta_*(t)$, then the function $I(\cdot)$ defined by (110) satisfies the following equation*

$$I(t) = \bar a(t,t-h)I(t-h) + o\big(h\big) \tag{115}$$

with $I(s) := I\big(\theta_p(s),\dot\theta_p(s),\theta_{0*},\dot\theta_{0*}\big)$ and

$$\bar a(t,t-h) := \exp\Big\{\int_{t-h}^t a(s)ds\Big\} \quad with \quad h>0,$$

where the function $a(\cdot)$ is defined in (112). ∎

The equation (115) is almost linear in terms of increment of the function $I(\cdot)$ over time step of length h, while the factor $\bar{a}(\cdot)$ is determined only by the nominal motion that have been chosen to stabilize. So that the iterating the equation (115) with small $h > 0$ for the time intervals to fill out the period T of the nominal oscillation $\theta_*(t)$ on sub-intervals

$$[0, h], \quad [h, 2h], \quad \ldots, \quad [T - h, T]$$

we obtain the relation

$$X_{k+1} = \mathcal{A}X_k + o(h) \tag{116}$$

with

$$X_k := \begin{bmatrix} I(T - h + kh) \\ I(T - 2h + kh) \\ \vdots \\ I(h + kh) \\ I(kh) \end{bmatrix} \tag{117}$$

and the constant matrix $\mathcal{A}$ defined as

$$\begin{bmatrix} \bar{a}(T, T - h) & 0 & \ldots & 0 \\ 0 & \bar{a}(T - h, T - 2h) & \ldots & 0 \\ \vdots & & & \vdots \\ 0 & \ldots & \bar{a}(2h, h) & 0 \\ 0 & \ldots & 0 & \bar{a}(h, 0) \end{bmatrix}$$

In turn, Eqn. (116) makes it possible to introduce into consideration new optimization problem as a tool for re-calibration of the model in the vicinity of nominal motion. Indeed, one can compute and improve the values of components of vectors (117) and the matrix $\mathcal{A}$ by searching for incremental updates of the current estimates of the parameters p_1-p_4 that minimize the error

$$\frac{1}{MT} \sum_{t}^{t+MT} \left\| \hat{X}_{k+1} - \widehat{\mathcal{A}}\hat{X}_k \right\|^2 \to \min \tag{118}$$

taken over sufficiently large number M of periods of the nominal motion.

Rationale behind posting new optimization problem for updating the present set of parameters is straightforward: *the behavior of the function (110) of the state of the closed loop system should obey such linear discrete*

time system with minor correction provided the parameters are known exactly; hence the parameters should be updated if the deviation from linear system is large! The correction assumes the minimization of the index (118) or the like.

5 Concluding remarks

The main focus of the thesis work has been paid to analysis and exemplification of numerical and experimental procedures of calibration of dynamics of robotic systems. For that purpose, we have followed the standard approach for searching resonance frequencies of mechanical system and reconstructing the system parameters based on their estimates if successfully computed such as in Eqn. (100). Having completed that steps, we have proposed an alternative to classical approach for calibration of some parameters of dynamics of robotic system, where instead of creating a generic model we would search for parametric and *linear* representation of a model in a vicinity of a nominal motion that the system should exhibit as accurate as possible. For that purpose, we have elaborated an example, where we found

- new quantity (invariant of the motion), see Eqn. (110), and
- the linear dynamical system (111) that this invariant should obey if the parameters for its computation are tuned accordingly.

In the case study, the procedure leads to the separation of the parameters on groups: p_4 appears as a coefficient in description of the linear dynamics, while p_1 and p_3 are required for computing the motion dependent invariant. The work has not been fully completed neither generalization have been proposed. However, we believe that some of arguments of the work become fresh and up to some extend new for the robotic applications. Furthermore, we hope that the work is just in the beginning and the industrial partner, who initiated the studies, will use the results and continue their exploration.

References

[1] Brunot M., A. Janot, P.C. Young, and F. Carrillo. "An improved instrumental variable method for industrial robot model identification," *Control Engineering Practice,* 74: 107-117, 2018.

[2] Casella, G. and Berger, R.L. (2002) Statistical Inference. 2nd Edition, Duxbury Press, Pacific Grove.

[3] Fradkov A.L. "Swinging control of nonlinear oscillations." *International J. Control*, 64(6): 1189-1202, 1996.

[4] Gaz C. and A. De Luca. "Payload estimation based on identified coefficients of robot dynamics - with application to collision detection," in *the Proceedings of IROS*, pp. 3033-3040, 2017.

[5] Goodwin G., S. Graebe, M. Salgado. "Control System Design." *Pearson,* 2001

[6] Hartman Ph. "Ordinary differential equations." *SIAM,* 1987.

[7] Hollerbach J., W. Khalil, and M. Gautier. "Model identification." In: *Springer Handbook of Robotics.* pp. 321–344, 2008.

[8] Khalil W. and E. Dombre. "Modeling, Identification and Control of Robots." *Butterworth-Heinemann.* 2004.

[9] Lee T., B.D. Lee, and F.C. Park. "Optimal excitation trajectories for mechanical system identification," *Automatica,* 131: paper No. 109773, 2021.

[10] Ljung L. "System Identification: Theory for user." *Prentice Hall,* 1999.

[11] Ziegler, J.G. and N.B. Nichols. "Optimum settings for automatic controllers" (PDF). Transactions of the ASME, 64: 759–768, 1942.

[12] Åstrom, K.J. and K. Furuta. "Swinging up a pendulum by energy control," in *the Proceedings of the 13th World Congress of IFAC,* Vol. E, pp. 37–42, 1996.

A MATLAB Code for Analysis

MATLAB scripts used for deriving the results are presented below, in addition data from the Butterfly Robot case study as well as Simulink models for the synthetic case explored in this thesis are posted here for public use: https://github.com/ArtemShiryaev/Thesis_Butterfly_Robot.

A.1 Synthetic case study

```
% Script 1
% Artem Angelchev Shiryaev
% MSc Thesis - August 2024
clc, close all, clear all

%% Step 0: Define the number of iterations and initialize storage
N = 5; % Define the number of iterations
Order_stat_all = cell(N,1); % Cell array to store order statistic from iteration
Order_stat_eq77 = cell(N,1);
raw_data_amp_omega = cell(N,1);


% initial conditions
th0 = 0.01; Dth0 = 0;

% true model parameters
M = 0.1; L = 0.05; Jc = 0.003; B = 10; g = 9.81; Kf = 0.001; p3 = B;
p1 = M*L^2 + Jc; p2 = M*L*g;
% Define initial values for p1 and p2
p1_initial = M*L^2 + Jc;
p2_initial = M*L*g;



% Mass and Length change each iteration
Mass_alpha = 0.05; %
Length_alpha = 0.005;


% Store values of Mass and Length alpha, p1,p2
Mass_alpha_values = zeros(N,1);
```

```
Length_alpha_values = zeros(N,1);
p1_values = zeros(N, 1);
p2_values = zeros(N, 1);

for iter = 1:N
    %% Step 1: Update p1 and p2
    % I vårt ex. p1 = p1, p2 = Kf, p3 = p2, p3 = p4
    p1 = p1_initial + (iter-1)*(Mass_alpha*(Length_alpha.^2) );
    p2 = p2_initial + (iter-1)*(Length_alpha*g*Mass_alpha);

    % Store values
    p1_values(iter) = p1;
    p2_values(iter) = p2;
    Mass_alpha_values(iter) = (iter-1)*Mass_alpha;
    Length_alpha_values(iter) = (iter-1)*Length_alpha;

    % Update the system transfer function with new p1 and p2
    sys = tf(p3,[p1 Kf p2]);

    %% Rest of your code remains the same
    % parameters of input sinusoid "A*sin( Om*t )"
    input_freq2 = 1:0.5:7; % rad/sec
    scales2 = [ones(length(input_freq2),1)]*1e-5;

    % generic parameters for running simulation
    step_size = 0.01; % step size for the solver
    T = 70;   % simulation time
    NNN = 1+(iter-1); % Internal paramater for eq 77 in simulink
    simIn2 = Simulink.SimulationInput("Model_of_pendulum_dynamics_for_SI_with_dr
    number_of_recorded_experiments = length(scales2);

    % Set up
    number_of_iterations2 = 1;
    Oms2 = zeros(number_of_recorded_experiments, number_of_iterations2);
    As2 = zeros(number_of_recorded_experiments, number_of_iterations2);
    seed_rand = 222;
    for NN = 1:number_of_recorded_experiments
        A_in2 = scales2(NN);
        Om_in2 = input_freq2(NN);
        for iteration = 1:number_of_iterations2
            %% Step 2: run synthetic experiment NN for generating the  data
```

```
            out = sim(simIn2);
            t2 = out.tout;
            u2 = out.u.Data;
        end
    end

    % Best function eq 77/79 (forbidden eq)
    data = [out.MnL.Data out.omega_opt.Data];
    data_unique = unique(data, 'rows', 'stable');
    Order_stat_eq77{iter} = data_unique;

    % (Optional) Display progress
    fprintf('Iteration %d completed with p1 = %.4f and p2 = %.4f\n', iter, p1, p
end


% Summary of eqn 77
temp_var = zeros(N,3);
for k=1:N
temp_var(k, :) = [Order_stat_eq77{k}(1,1) Order_stat_eq77{k}(1,2) Order_stat_eq7
end
summary_table2 = array2table(temp_var,'VariableNames', {'Mass alpha', 'Length al
disp(summary_table2)


%% same script with old values
clearvars -except summary_table2 N


%% Step 1: initialize the Simulink model

% initial conditions
th0 = 0.01; Dth0 = 0;

% true model parameters
M = 0.1; L = 0.05; Jc = 0.003; B = 10; g = 9.81; Kf = 0.001;

% saving optimal omega


Num123 = N;
```

```
114 Omega_opt_eq100 = zeros(Num123,1);
115 Alpha_Values = zeros(Num123,2);
116 for kk=1:Num123
117 Mass_alpha = 0.05*(kk -1); %
118 Length_alpha = 0.005*(kk -1);
119 Alpha_Values(kk,:) = [Mass_alpha Length_alpha];
120
121 p1 = M*L^2 + Jc + Mass_alpha*Length_alpha^2 ; p2 = M*L*g + Mass_alpha*g*Length_a
122 %p1 = Jc + M*(L^2)
123 %p2 = Kf + Kemf*(Ki/R)
124 %p3 = M*g*L
125 %p4 = Ki/R
126
127 % I vårt ex. p1 = p1, p2 = Kf, p3 = p2, p3 = p4
128 sys = tf(p3,[p1 Kf p2]);
129
130 % parameters of input sinusoid "A*sin( Om*t )"
131 input_freq = [1, 1.5,  2, 2.5,  3, 3.5,  4, 4.5,  5, 5.5,  6, 6.5,  7]; % rad/se
132 scales = [1,   1,  1,   1,  1,   1,  1,   1,  1,   1,  1,   1,  1]*1e-5;
133
134
135
136 % generic parameters for running simulation
137 step_size = 0.01; % step size for the solver
138 T = 70;   % simulation time
139 %simIn = Simulink.SimulationInput("Model_of_pendulum_dynamics_for_SI");
140 simIn = Simulink.SimulationInput("Model_of_pendulum_dynamics_for_SI_with_dryfric
141 number_of_recorded_experiments = length(scales);
142
143 % Set up
144 number_of_iterations = 1;
145 Oms = zeros(number_of_recorded_experiments, number_of_iterations);
146 As = zeros(number_of_recorded_experiments, number_of_iterations);
147
148
149 seed_rand = 222;
150
151 for NN = 1:number_of_recorded_experiments
152     A_in = scales(NN);
153     Om_in = input_freq(NN);
154     for iteration = 1:number_of_iterations
```

```
155         %% Step 2: run synthetic experiment NN for generating the  data
156         out = sim(simIn);
157         t = out.tout;
158         u = out.u.Data;
159         q = out.q.Data; % data are: time "t", input "u", angle "q"
160
161         %% Add noise to the input signal
162         seed_rand = 222*iteration;
163
164
165         %% Step 3: visualize the input signal
166         u_max = max(u);
167         frequency_of_input_signal = input_freq(NN);
168         %figure(1), plot(t,u), grid on, xlabel('time (sec)'), ylabel('control in
169         %ttl = strcat('Control input to the system is a sinusoid of amplitude ',
170         %title(ttl);
171         %ylim([-u_max*1.1, u_max*1.1]);
172
173         %% Step 4: visualize the irregularity of sampling
174         dt = zeros(size(t));
175         dt(1:end-1) = t(2:end);
176         dt = dt - t;
177         dt(end)=[];
178         dt_mean = mean(dt);      % <- the average of the sampling steps
179         %figure(2), plot(dt(1:end),'o'), hold on, plot(ones(length(dt),1)*dt_mea
180         %title('Intervals between samples is varying; the mean value of sampling
181
182         %% Step 5: resample and visualize the recorded values of the angle with
183         q_original = timeseries(q,t);
184         uniform_step_size = ( t(end) - t(1) )/( length(t)-1);
185         t_with_equally_distributed_sampling = (t(1):uniform_step_size:t(end))';
186         q_temp = resample(q_original, t_with_equally_distributed_sampling);
187         q_with_equally_distributed_sampling = q_temp.Data;
188
189         new_step_size = 4;       % this variable defines new step size for resam
190         q_resampled = q_with_equally_distributed_sampling(1:new_step_size:end);
191         t_resampled = t_with_equally_distributed_sampling(1:new_step_size:end);
192
193         %figure(3), plot(t,q,'b-'), hold on;
194         %figure(3), plot(t_resampled,q_resampled,'r.'), hold off;
195         %title('Comparison of the original and resampled signal');
```

```
196
197         %% Step 6: ignore the data that correspond to transition to the steady-s
198         XX = 45;
199         dt_r = t_resampled(2) - t_resampled(1);
200         q_steady_state_r = q_resampled( length(q_resampled)-floor(XX/dt_r):end )
201         t_steady_state_r = t_resampled( length(q_resampled)-floor(XX/dt_r):end )
202
203         q_steady_state = q_with_equally_distributed_sampling( length(q_with_equa
204         t_steady_state = t_with_equally_distributed_sampling( length(t_with_equa
205
206         %figure(4), plot( t_steady_state_r, q_steady_state_r , 'ro' ),  hold on;
207         %figure(4), plot( t_steady_state,   q_steady_state , 'b.' ),  grid on, h
208         %xlabel('time (sec)'), ylabel('q (rad)'), title('Steady state behavior o
209
210         %% Step 7: analyze the time response of the (resampled) angle values by
211         y = fft(q_steady_state_r');
212         y(1) = [];
213         n = length(y);
214         power = abs( y(1:floor(n/2)) ).^2;     % power of first half of transfor
215         maxfreq = 1/dt_r*(1/2);                 % maximum frequency
216         freq = (1:n/2)/(n/2)*maxfreq*2*pi;  % range of frequencies measured in r
217
218         %figure(5), plot(freq, power,'r.-'), grid on, xlim([0.1 max(input_freq)+
219         %xlabel('frequency \omega (rad/sec)'), ylabel('power (dimensionless)'),
220         %title('Periodogram of the steady state response');
221
222         %% Step 8: observe that the system response is approximately a sinusoid;
223         [max_of_power_spectrum,ind] = max(power);
224         Om = freq(ind);    % the dominant frequency of the response
225
226         %% Step 9: computing an estimate for the amplitude of frequency response
227         % compute and remove the mean for the original data for the last XX seco
228         min_value = min(q_steady_state_r);
229         max_value = max(q_steady_state_r);
230         q_ss_mean = (max_value + min_value)/2;
231         q_ss_centred = q_steady_state_r - q_ss_mean;
232
233         %figure(10), plot(t_steady_state_r, q_ss_centred,'o' ), grid on;
234
235         q2_ss_centered = abs(q_steady_state  - q_ss_mean ).^2;
236         %figure(11), plot(t_steady_state,  q2_ss_centered , '.b' ), grid on;
```

```
237
238         % estimate 1: if the response would be indeed a sine of frequency "Om" t
239         A2 = sqrt(2)*sqrt( sum(q2_ss_centered) )*sqrt(uniform_step_size/XX);
240         new_sin = A2*sin( Om*t_steady_state);
241         %figure(10), hold on, plot(t_steady_state,new_sin,'g-','LineWidth',2), h
242
243         Oms(NN, iteration) = Om;
244         As(NN, iteration) = 20*log10(A2/scales(NN));
245     end
246 end
247
248
249 %% New section
250 temp_variable = As;
251 temp_variable_max = max(temp_variable);
252 temp_variable_max2 = max(temp_variable(temp_variable<max(temp_variable)));
253
254 temp_variable2 = [As, Oms];
255
256 [MM, Index] = max(temp_variable2);
257 Max__2 = [temp_variable2(Index(1),1), temp_variable2(Index(1),2)];
258 Max__2;
259
260 [MM2, Index2] = max(temp_variable(temp_variable<max(temp_variable)));
261 Max__3 = [temp_variable2(Index2(1),1), temp_variable2(Index2(1),2)];
262 Max__3;
263
264
265 Largest_Oms_As = [Max__2;Max__3];
266
267
268 % testing the new methods
269 % a_0 = p3/p1, a_1 = p2/p1
270 A__0 = p2/p1;
271 A__1 = Kf/p1;
272
273
274 Omg_out = sqrt(A__0 - (A__1.^2)/2);
275 % Omg_out = 3.8788
276
277 Omg_out2 = sqrt(M*g*L/(Jc + M*(L^2)) - ((((Kf + B)^2)/2*((Jc + M*(L^2))^2))));
```

```
278 % Omg_out2 = 3.8848
279
280 %% Omega Opt
281 g_K = Largest_Oms_As(1,1);
282 g_K1 = Largest_Oms_As(2,1);
283 omega_gK = Largest_Oms_As(1,2);
284 omega_gK1 = Largest_Oms_As(2,2);
285 Omega_opt_eq100(kk) = sqrt((omega_gK^2 * sqrt((g_K1^2 / g_K^2) + 1) + omega_gK1^
286
287 fprintf('Iteration %d completed with p1 = %.4f and p2 = %.4f\n', kk, p1, p2);
288
289 end
290
291
292 summary_data = [Alpha_Values Omega_opt_eq100];
293 summary_table = array2table(summary_data);
294 summary_table.Properties.VariableNames = {'Mass alpha', 'Length alpha', 'Optimal
295
296
297 clearvars -except summary_table summary_table2 Kf N
298
299 disp(summary_table)
300 disp(summary_table2)
301
302 %% Optimzation of paramaters
303
304 %% Compute p1,p3
305 data = [table2array(summary_table2) table2array(summary_table(:,3))];
306
307 data_table = array2table(data);
308 data_table.Properties.VariableNames = {'Mass alpha', 'Length alpha','Optimal Ome
309
310 disp(data_table)
311
312
313 % Constants
314 Kf = 0.001;
315 p2 = Kf;
316 M = 0.1; L = 0.05; Jc = 0.003; g = 9.81; Kf = 0.001;
317
318 % Objective function to minimize
```

```
objective_function = @(params) compute_f(params, data, g, p2);

% Initial guess for p1 and p3
initial_guess = [(M*L^2 + Jc)*0.5, (M*L*g)*0.5];

% Define lower and upper bounds for p1 and p3
lb = [0, 0]; % Lower bounds
ub = [1,1];
%ub = [(M*L^2 + Jc)*5, (M*L*g)*5]; % Upper bounds

% Perform optimization using fmincon with bounds
options = optimoptions('fmincon','Display','iter'); % Show iteration information
estimated_params = fmincon(objective_function, initial_guess, [], [], [], [], lb

% Display the estimated parameters
disp('Estimated p1 and p3:');
disp(estimated_params);

real_params = [(M*L^2 + Jc) M*L*g];
disp('Real p1 and p3:');
disp(real_params)

temp_residuals = real_params - estimated_params;
disp('Estimated Residual p1 and p3:');
disp(temp_residuals)


%% Compute p1,p2,p3

% Initial guess for p1, p2, and p3
initial_guess2 = [(M*L^2 + Jc)*0.5, 0.001*0.5, (M*L*g)*0.5]; % Adjusted for p1,

% Define lower and upper bounds for p1, p2, and p3
lb2 = [0, 0, 0]; % Lower bounds for p1, p2, and p3
ub2 = [(M*L^2 + Jc)*10, 0.001*10, (M*L*g)*10]; % Upper bounds for p1, p2, and p3

% Objective function to minimize
objective_function2 = @(params) compute_ff(params, data, g);

% Perform optimization using fmincon with bounds
options2 = optimoptions('fmincon', 'Display', 'iter'); % Show iteration informat
```

```
360 estimated_params2 = fmincon(objective_function2, initial_guess2, [], [], [], [],
361
362 % Display the estimated parameters
363 disp('Estimated p1, p2, and p3:');
364 disp(estimated_params2);
365
366 real_params2 = [(M*L^2 + Jc), 0.001, M*L*g];
367 disp('Real p1, p2, and p3:');
368 disp(real_params2)
369
370 temp_residuals2 = real_params2 - estimated_params2;
371 disp('Residuals for p1, p2, and p3:');
372 disp(temp_residuals2)
373
374
375
376 %% Function to compute f(p1, p3)
377 function f_value = compute_f(params, data, g, p2)
378     p1 = params(1);
379     p3 = params(2);
380
381     % Initialize the sum
382     f_value = 0;
383
384     % Loop over the data points
385     for i = 1:size(data, 1)
386         m_a_k = data(i, 1);
387         l_a_n = data(i, 2);
388         omega_opt = data(i, 4); % Use the Omega from eq 100
389
390         % Calculate the left side of the equation (Omega opt squared)
391         omega_opt_sq = omega_opt^2;
392
393         % Calculate the right side of the equation
394         term1 = (p3 + m_a_k * g * l_a_n) / (p1 + m_a_k * l_a_n^2);
395         term2 = (1/2) * (p2^2) / (p1 + m_a_k * l_a_n^2)^2;
396         right_side = term1 - term2;
397
398         % Sum of squared differences
399         f_value = f_value + abs((omega_opt_sq - right_side))^2;
400     end
```

```
end

%% Function to compute f(p1, p2, p3)
function f_value2 = compute_ff(params, data, g)
    p1 = params(1);
    p2 = params(2);
    p3 = params(3);

    % Initialize the sum
    f_value2 = 0;

    % Loop over the data points
    for i = 1:size(data, 1)
        m_a_k = data(i, 1);
        l_a_n = data(i, 2);
        omega_opt = data(i, 4); % Use the Omega from eq 100

        % Calculate the left side of the equation (Omega opt squared)
        omega_opt_sq = omega_opt^2;

        % Calculate the right side of the equation
        term1 = (p3 + m_a_k * g * l_a_n) / (p1 + m_a_k * l_a_n^2);
        term2 = (1/2) * (p2^2) / (p1 + m_a_k * l_a_n^2)^2;
        right_side = term1 - term2;

        % Sum of squared differences
        f_value2 = f_value2 + abs((omega_opt_sq - right_side))^2;
    end
end
```

A.2 Butterfly Robot case study

```
% Script 2
% Artem Angelchev Shiryaev
% MSc Thesis - August 2024

clc;
close all;
```

```
clear all;

% Define the datasets
datasets = {'52 grams', '120.5 grams', '154 grams'};

% Initialize results storage
Omega_opt_eq100_results = zeros(length(datasets), 1);

% Loop over each dataset
for ds = 1:length(datasets)

    %% Step 1: Initialize Parameters and Read Data File Names

    % Select the data set
    data_set = datasets{ds};

    % Define scales, input frequencies, and file path based on the selected data
    switch data_set
        case '52 grams'
            scales = [0.008, 0.008, 0.006, 0.005, 0.003, 0.003, 0.003, 0.004, 0.
            input_freq = [2, 2.5, 3, 3.5, 4, 4.5, 5, 5.5, 6, 8, 10, 12, 14, 16];
            path_to_data = 'C:\Users\Artem\Desktop\Matlab_code\52gmat\';
        case '120.5 grams'
            scales = [0.015, 0.01, 0.01, 0.01, 0.01, 0.008, 0.004, 0.003, 0.006,
            input_freq = [3, 3.5, 4, 4.5, 4.75, 5, 5.5, 6, 6.5, 7, 9, 11, 13, 15
            path_to_data = 'C:\Users\Artem\Desktop\Matlab_code\120_5gmat\';
        case '154 grams'
            scales = [0.015, 0.015, 0.015, 0.008, 0.004, 0.003, 0.006, 0.01, 0.0
            input_freq = [3.5, 4, 4.5, 5, 5.5, 6, 6.5, 7, 7.5, 8, 10, 12, 14];
            path_to_data = 'C:\Users\Artem\Desktop\Matlab_code\154gmat\';
        otherwise
            error('Invalid data set selected.');
    end

    % Read names of data files
    names_of_data_files_as_a_cell = read_file_names(path_to_data);
    number_of_recorded_experiments = length(names_of_data_files_as_a_cell{1});

    % Initialize storage for results
    As = zeros(number_of_recorded_experiments, 1);
    Oms = zeros(number_of_recorded_experiments, 1);
```

```
48      Order_stat_all = cell(number_of_recorded_experiments, 1);
49      raw_data_amp_omega = cell(number_of_recorded_experiments, 1);
50
51      %% Analysis part
52      for NN = 1:number_of_recorded_experiments
53
54          %% Step 2: Load real experiment data
55          currently_loaded_file = fullfile(path_to_data, names_of_data_files_as_a_
56          load(currently_loaded_file, 'D');
57
58          % Extract data
59          t = D(:, 1);
60          u = D(:, 2);
61          q = D(:, 3);
62          dq = D(:, 4); % data are: time "t", input "u", angle "q", angular veloci
63
64
65
66          %% Step 4: Analyze sampling irregularity
67          dt = diff(t);
68          dt_mean = mean(dt);      % <- the average of the sampling steps
69
70          %% Step 5: Resample the recorded values of the angle with the new sampli
71          q_original = timeseries(q, t);
72          uniform_step_size = (t(end) - t(1)) / (length(t) - 1);
73          t_with_equally_distributed_sampling = (t(1):uniform_step_size:t(end))';
74          q_temp = resample(q_original, t_with_equally_distributed_sampling);
75          q_with_equally_distributed_sampling = q_temp.Data;
76
77          new_step_size = 25; % This variable defines new step size for resampled
78          q_resampled = q_with_equally_distributed_sampling(1:new_step_size:end);
79          t_resampled = t_with_equally_distributed_sampling(1:new_step_size:end);
80
81          %% Step 6: Consider only the last XX seconds of steady-state behavior
82          XX = 30;
83          dt_r = t_resampled(2) - t_resampled(1);
84
85          q_steady_state_r = q_resampled(max(1, length(q_resampled) - floor(XX/dt_
86          t_steady_state_r = t_resampled(max(1, length(t_resampled) - floor(XX/dt_
87
88          %% Step 7: Analyze the time response of the (resampled) angle values by
```

```
        y = fft(q_steady_state_r');
        y(1) = [];
        n = length(y);
        power = abs(y(1:floor(n/2))).^2; % Power of first half of transform data
        maxfreq = 1/dt_r*(1/2); % Maximum frequency
        freq = (1:n/2)/(n/2)*maxfreq*2*pi; % Range of frequencies measured in ra

        %% Step 8: Compute dominant frequency and estimate amplitude
        [max_of_power_spectrum, ind] = max(power);
        Om = freq(ind); % The dominant frequency of the response

        min_value = min(q_steady_state_r);
        max_value = max(q_steady_state_r);
        q_ss_mean = (max_value + min_value) / 2;
        q_ss_centred = q_steady_state_r - q_ss_mean;

        q2_ss_centered = abs(q_ss_centred).^2;
        A2 = sqrt(2) * sqrt(sum(q2_ss_centered)) * sqrt(uniform_step_size / XX);

        Oms(NN) = Om;
        As(NN) = 20*log10(A2 / scales(NN));

        data_amp_omega = [Oms, As];
        raw_data_amp_omega{NN} = data_amp_omega;
        Order_stat = sortrows(data_amp_omega, -2);
        Order_stat_all{NN} = Order_stat;
    end

    %% Step 9: Compute Omega Opt based on eq 100
    sqrd_omega_gK = (Order_stat_all{number_of_recorded_experiments}(1,1)).^2;
    sqrd_omega_gK1 = (Order_stat_all{number_of_recorded_experiments}(2,1)).^2;
    sqrd_g_K = (Order_stat_all{number_of_recorded_experiments}(1,2)).^2;
    sqrd_g_K1 = (Order_stat_all{number_of_recorded_experiments}(2,2)).^2;

    Omega_opt_eq100 = sqrt((sqrd_omega_gK * sqrt((sqrd_g_K1 / sqrd_g_K) + 1) + s
        / (sqrt((sqrd_g_K1 / sqrd_g_K) + 1) + sqrt(2)));

    % Store the result for the current dataset
    Omega_opt_eq100_results(ds) = Omega_opt_eq100;

    % Display results for the current dataset
```

```
    fprintf('Optimal Omega for %s: %.4f\n', data_set, Omega_opt_eq100);

end

%% Display All Results
disp('Optimal Omega for all datasets:');
for ds = 1:length(datasets)
    fprintf('%s: %.4f\n', datasets{ds}, Omega_opt_eq100_results(ds));
end

%% Constrained Optimization for p1,p2,p3

% Prepare the data
data = [0.052, 0.1205,0.154; % mass in kg
        0.104, 0.104,0.104;     % length in cm
        4.1889, 5.7606,6.281;]';% optimal omega based on eq 100


% Constants approximate from experience
M = 0.2;
L = 0.104;
Jc = 0.003;
g = 9.81;

% Initial guess for p1, p2, and p3
initial_guess = [(M*L^2 + Jc)*0.5, 0.001*0.5, (M*L*g)*0.5]; % Adjusted for p1, p

% Define lower and upper bounds for p1, p2, and p3
lb = [0, 0, 0]; % Lower bounds for p1, p2, and p3
ub = [(M*L^2 + Jc)*20, 0.001*20, (M*L*g)*20]; % Upper bounds for p1, p2, and p3

% Objective function to minimize
objective_function = @(params) compute_f(params, data, g);

% Perform optimization using fmincon with bounds
options = optimoptions('fmincon', 'Display', 'iter'); % Show iteration informati
estimated_params = fmincon(objective_function, initial_guess, [], [], [], [], lb

% Display the estimated parameters
disp('Estimated p1, p2, and p3:');
disp(estimated_params);
```

```
171
172
173 %% Function to compute f(p1, p2, p3)
174 function f_value = compute_f(params, data, g)
175     p1 = params(1);
176     p2 = params(2);
177     p3 = params(3);
178
179     % Initialize the sum
180     f_value = 0;
181
182     % Loop over the data points
183     for i = 1:size(data, 1)
184         m_a_k = data(i, 1);
185         l_a_n = data(i, 2);
186         omega_opt = data(i, 3); % Use the Omega from eq 100
187
188         % Calculate the left side of the equation (Omega opt squared)
189         omega_opt_sq = omega_opt^2;
190
191         % Calculate the right side of the equation
192         term1 = (p3 + m_a_k * g * l_a_n) / (p1 + m_a_k * l_a_n^2);
193         term2 = (1/2) * (p2^2) / (p1 + m_a_k * l_a_n^2)^2;
194         right_side = term1 - term2;
195
196         % Sum of squared differences
197         f_value = f_value + abs((omega_opt_sq - right_side))^2;
198     end
199 end
200
201 %% Reading data function
202 function A = read_file_names(path_to_data)
203     % Returns the list of names of files stored in the directory
204     listed_files_names = fullfile(path_to_data, 'file_names.txt');
205     fileID = fopen(listed_files_names, 'r');
206     if fileID == -1
207         error('File not found: %s', listed_files_names);
208     end
209     formatSpec = '%s';
210     A = textscan(fileID, formatSpec);
211     fclose(fileID);
```

```
212 end
```

UMEÅ UNIVERSITY

Department of Mathematics and Mathematical Statistics
SE-901 87 Umeå www.umu.se/en/math